© 2015. Published by The Company of Biologists Ltd | Development (2015) 142, 1006-1015 doi:10.1242/dev.120618

RESEARCH ARTICLE

Extramacrochaetae functions in dorsal-ventral patterning of *Drosophila* imaginal discs

Carrie M. Spratford[1,2] and Justin P. Kumar[1,*]

ABSTRACT

One of the seminal events in the history of a tissue is the establishment of the anterior-posterior, dorsal-ventral (D/V) and proximal-distal axes. Axis formation is important for the regional specification of a tissue and allows cells along the different axes to obtain directional and positional information. Within the *Drosophila* retina, D/V axis formation is essential to ensure that each unit eye first adopts the proper chiral form and then rotates precisely 90° in the correct direction. These two steps are important because the photoreceptor array must be correctly aligned with the neurons of the optic lobe. Defects in chirality and/or ommatidial rotation will lead to disorganization of the photoreceptor array, misalignment of retinal and optic lobe neurons, and loss of visual acuity. Loss of the helix-loop-helix protein Extramacrochaetae (Emc) leads to defects in both ommatidial chirality and rotation. Here, we describe a new role for *emc* in eye development in patterning the D/V axis. We show that the juxtaposition of dorsal and ventral fated tissue in the eye leads to an enrichment of *emc* expression at the D/V midline. *emc* expression at the midline can be eliminated when D/V patterning is disrupted and can be induced in situations in which ectopic boundaries are artificially generated. We also show that *emc* functions downstream of Notch signaling to maintain the expression of *four-jointed* along the midline.

KEY WORDS: Eye, Retina, Dorsoventral patterning, Extra macrochaetae, Notch, Four-jointed

INTRODUCTION

Complex organs such as the mammalian retina are composed of several distinct functional units and hundreds, if not thousands, of different cell types. During development several mechanisms are put in place to ensure that each cell knows its exact geographical position so that it will adopt the appropriate fate for its location. A reliable piece of positional information is the relative location of each cell along three major axes: anterior-posterior, dorsal-ventral (D/V) and proximal-distal. Each axis serves as a signaling center that influences cell fate choices across the developing tissue by secreting short- and long-range morphogens. Cells that lie at varying distances from each axis must interpret the relative intensity of each signal and activate appropriate gene expression programs. Failure to specify each axis or to generate the polarizing signals that emanate from these singling centers can have catastrophic effects on organ development and function. Here, we use the *Drosophila* eye to examine the role that the helix-loop-helix (HLH) protein Extramacrochaetae (Emc) plays in patterning across the D/V axis.

The adult eye contains ∼750 unit eyes, or ommatidia, that are evenly placed within dorsal and ventral compartments. Each ommatidium contains eight photoreceptors (R1-8) that appear as an asymmetric trapezoid, with the R3 and R4 cells occupying unbalanced positions within the unit (Dietrich, 1909; Chen, 1929; Waddington and Perry, 1960). The ommatidia in the dorsal and ventral halves are mirror images of each other and where they meet in the adult retina is referred to as the equator (Ready et al., 1976). In order to generate these mirror-image arrangements, the photoreceptor clusters must first adopt different chiralities and then rotate in opposite directions. D/V patterning in the developing eye takes place during the larval stages and can be divided into early and late phases. In the early phase (late first/early second instar) the unpatterned eye is subdivided into dorsal, ventral, and midline compartments. In the latter phase (third instar), ommatidia adopt the correct chirality and rotate in the direction that is appropriate for their location in either the dorsal or ventral compartment.

In nearly all imaginal discs, the D/V axis is laid down during the late first/early second larval instar (Bohn, 1967; Bryant, 1970; Garcia-Bellido and Merriam, 1971a,b; Lawrence and Morata, 1976; Williams et al., 1993). Prior to the imposition of dorsal identity, the entire eye disc expresses the ventral selector gene *fringe* (*fng*). During the late first/early second instar, expression of *pannier* (*pnr*), which encodes a GATA transcription factor, is activated via an unknown mechanism in a small group of cells within the peripodial membrane along the dorsal margin (Heitzler et al., 1996; Maurel-Zaffran and Treisman, 2000; Oros et al., 2010). Pnr is then responsible for inducing the expression of *wingless* (*wg*) (Maurel-Zaffran and Treisman, 2000), which in turn activates expression of the Iroquois complex (Iro-C) genes within the dorsal half of the eye (McNeill et al., 1997; Heberlein et al., 1998). One member of Iro-C, *mirror* (*mirr*), represses the expression of *fng* in the dorsal half of the eye field (Cho and Choi, 1998; Cavodeassi et al., 1999; Yang et al., 1999; Sato and Tomlinson, 2007). In the ventral half of the eye, *sloppy paired 1* (*slp1*) represses *mirr*, which in turn preserves *fng* expression and ventral identity (Sato and Tomlinson, 2007). The confrontation of *fng*$^{-}$ (dorsal) and *fng*+ (ventral) tissue leads to the differential activation of *Delta* (*Dl*) and *Serrate* (*Ser*) within the two compartments and the activation of Notch (N) signaling at the D/V midline (Panin et al., 1997; Cho and Choi, 1998; Dominguez and de Celis, 1998; Papayannopoulos et al., 1998). Notch signaling at the midline is necessary for the growth of the eye field and for the expression of *four-jointed* (*fj*) (Zeidler et al., 1999; Chao et al., 2004; Reynolds-Kenneally and Mlodzik, 2005; Gutierrez-Aviño et al., 2009). Fj has been linked to planar cell polarity (PCP) and for Notch- and JAK/STAT-dependent growth (Zeidler et al., 1999; Gutierrez-Aviño et al., 2009). Thus, the early division of the eye into dorsal, ventral and midline zones is

[1]Department of Biology, Indiana University, Bloomington, IN 47405, USA.
[2]Department of Molecular, Cell, and Developmental Biology, University of California, Los Angeles, Los Angeles, CA 90095, USA.

*Author for correspondence (jkumar@indiana.edu)

Received 2 December 2014; Accepted 15 January 2015

Development (2015) 142, 1006-1015 doi:10.1242/dev.120618

important for growth and for providing relevant positional information for later chirality and rotation decisions.

The second phase of D/V patterning occurs during the third larval instar as neuronal specification takes place behind the morphogenetic furrow. The early ommatidium is symmetrical with respect to the position of the presumptive R3 and R4 cells. The presumptive R3 lies on the equatorial side of the photoreceptor cluster, while the R4 lies on the polar side (Ready et al., 1976; Tomlinson and Ready, 1987). This symmetry is broken by the activity of several factors, including the Frizzled (Fz) receptor and the Notch signaling pathway. Fz levels are maintained at higher levels in the presumptive R3 cell as compared with the R4 precursor and are required to translate different levels of an as yet unidentified ligand into distinct gene expression programs (Zheng et al., 1995; Tomlinson and Struhl, 1999). Elevated Fz in the R3 precursor induces the production of Dl, which in turn activates the Notch pathway in the neighboring R4 precursor (Cooper and Bray, 1999; Fanto and Mlodzik, 1999). As a result, the R3 and R4 photoreceptors are now functionally distinct from each other. Ommatidia mutant for *fz* exhibit defects in chirality as well as in the direction and degree of rotation. In many *fz* mutant ommatidia, the R4 precursor adopts an R3 fate (Zheng et al., 1995). Likewise, in ommatidia with reduced Notch signaling, both precursors adopt the R3 fate, whereas hyperactivation of the pathway induces both cells to adopt the R4 fate (Cooper and Bray, 1999; Fanto and Mlodzik, 1999; Tomlinson and Struhl, 1999). Thus, maintaining appropriate levels of Fz and Notch activity in the R3/4 photoreceptor pair is crucial for the establishment of PCP in the eye.

Two additional factors that influence PCP are the transmembrane cadherins Fat (Ft) and Dachsous (Ds) (Mahoney et al., 1991; Clark et al., 1995; Ishikawa et al., 2008). These proteins affect PCP in part by maintaining higher Fz receptor levels in the presumptive R3 cell as compared with the R4 precursor (Yang et al., 2002). *ft* is expressed in a relatively uniform pattern throughout the eye disc, whereas *ds* is expressed in a gradient with highest levels at the poles. Mutations in the Fat/Ds system cause strong PCP defects throughout the entire disc (Yang et al., 2002; Rawls et al., 2002; Simon, 2004; Brittle et al., 2012; Thomas and Strutt, 2012; Sharma and McNeill, 2013; Ayukawa et al., 2014). By contrast, the eyes of homozygous loss-of-function *fj* mutant alleles are characterized by relatively weak PCP defects (Zeidler et al., 1999). Although mutant *fj* clones show somewhat stronger phenotypes, including non-autonomous effects (Zeidler et al., 1999), these are still relatively mild compared with disruptions of the Ft/Ds or Fz/Notch systems.

Once the R3/4 cells have adopted their individual fates, their positions in relation to each other will shift slightly, thus breaking the symmetry of the photoreceptor cluster. Ommatidia in the dorsal and ventral halves of the eye then rotate 90° in opposite directions, forming a mirror image across the equator. Rotation is a two-step process: there is an initial 45° rotation followed by a pause for 3-4 columns (~6-8 h), and then a second 45° rotation (Choi and Benzer, 1994). Fz regulates the expression of one rotation gene, *nemo*, suggesting that there is a molecular connection between PCP and rotation (Zheng et al., 1995).

Emc encodes an HLH protein that binds and forms heterodimers with several basic HLH (bHLH) proteins, including Daughterless (Da) and members of the Achaete-Scute complex (AS-C) (Garrell and Modolell, 1990; Ellis et al., 1990; van Doren et al., 1991, 1992; Alifragis et al., 1997). Since Emc lacks the basic DNA-binding domain, neither Emc itself nor Emc-bHLH heterodimers can interact with DNA (van Doren et al., 1991, 1992). Therefore, Emc functions to sequester bHLH proteins away from their target genes. Retinas lacking *emc* suffer from several developmental defects, including disruptions in PCP and ommatidial rotation (Brown et al., 1995; Bhattacharya and Baker, 2009). The latter report demonstrated that, despite the loss of *emc*, the vast majority of R3/4 cells are specified correctly and that Notch signaling appears normal in the R4 cell. Based on these observations, it can be concluded that although *emc* is expressed in the R3/4 pair it is unlikely that the PCP and rotation defects seen in *emc* mutants are due to the loss of *emc* in these cells.

In a prior report, we have shown that *emc* expression is enriched along the D/V midline (Spratford and Kumar, 2013). This enrichment persists at the midline ahead of the advancing furrow even in late third instar discs (Brown et al., 1995; Bhattacharya and Baker, 2009; Spratford and Kumar, 2013). Here we demonstrate that Emc does not play a role in establishing the D/V midline but rather is expressed here in response to the formation of the midline. We also show that *emc* lies downstream of N signaling to regulate *fj* expression at the midline. Prior reports had demonstrated that Notch signaling regulates *fj* expression (Zeidler et al., 1999; Gutierrez-Aviño et al., 2009) and the implicit model has been that Notch signaling via Suppressor of Hairless [Su(H)] directly regulates *fj* expression. Our data support an alternative model in which Notch pathway activation of *emc* is required to maintain *fj* expression at the midline. Since relatively weak PCP phenotypes are seen in *fj* mutant retinas (Zeidler et al., 1999; Strutt et al., 2003), our data suggest that Emc influences PCP by also regulating other factors throughout the eye field. These factors are likely to lie outside of the Ft/Ds system, as *ds* expression is normal in *emc* loss-of-function clones. One potential target of Emc is likely to be the Wg pathway, as we have previously shown the Emc regulates *wg* transcription along the ventral margin (Spratford and Kumar, 2013). Our results indicate that Emc functions in both the early and late phases of D/V patterning.

RESULTS

emc expression is enriched at the midline of the *Drosophila* eye

In their seminal report on the role that Emc plays in eye development, Brown and colleagues reported that retinal clones of a hypomorphic *emc* mutant allele (emc^{1}) display slight PCP defects (Brown et al., 1995). A subsequent report using an *emc* null allele (emc^{AP6}) showed that ommatidia also fail to rotate correctly when the entire eye is mutant for *emc* (Bhattacharya and Baker, 2009). To study the mechanism by which Emc influences D/V patterning we first determined the expression pattern of *emc* in the eye, using a polyclonal antibody that recognizes Emc protein and six enhancer trap lines (four *GFP* and two *lacZ* insertions) that are located within 822 bp upstream of the transcriptional start site. We found that all six transcriptional reporters show expression throughout the entire disc as well as substantial enrichment along the D/V midline (Fig. 1A,B) (Spratford and Kumar, 2013). The transcriptional reporters are likely to provide an accurate view of *emc* expression since the antibody also reveals an enrichment of Emc protein at the midline (Fig. 1C).

The strikingly high midline expression that is revealed by the enhancer traps suggested that the GFP and *lacZ* reporters are under the control of a nearby D/V midline-specific enhancer element. In an attempt to identify this enhancer, we cloned 4 kb of DNA upstream of the transcriptional start site (surrounding the insertion sites of all six enhancer traps) but, unfortunately, several fragments containing portions of the upstream DNA sequence failed to drive expression of a *lacZ* reporter at the midline (supplementary material

Development (2015) 142, 1006-1015 doi:10.1242/dev.120618

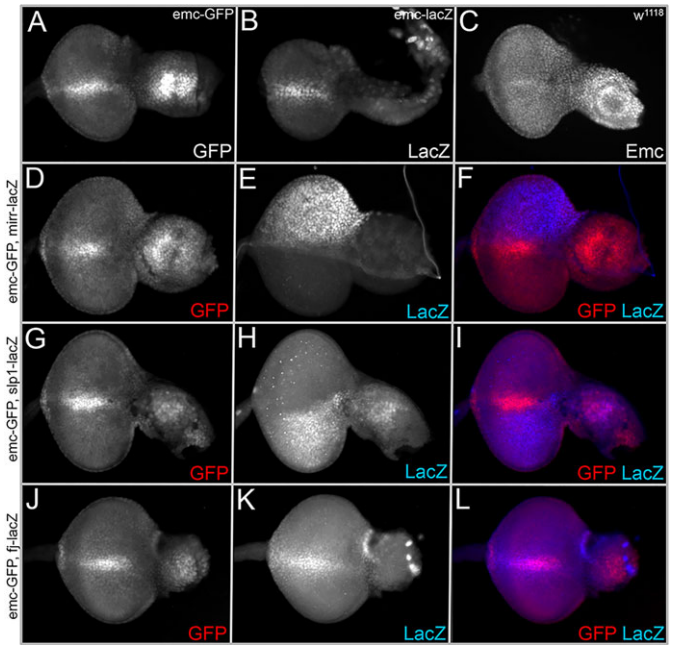

Fig. 1. *emc* is expressed along the D/V midline of the developing *Drosophila* eye. (A-C) *emc-GFP*, *emc-lacZ* and Emc protein are enriched at the midline of early third instar eye imaginal discs. (D-I) *emc-GFP* at the midline lies between *mirr-lacZ* and *slp1-lacZ* domains. (J-L) *emc-GFP* and *fj-lacZ* patterns overlap significantly at the D/V midline. Dorsal side is up and anterior is to the right.

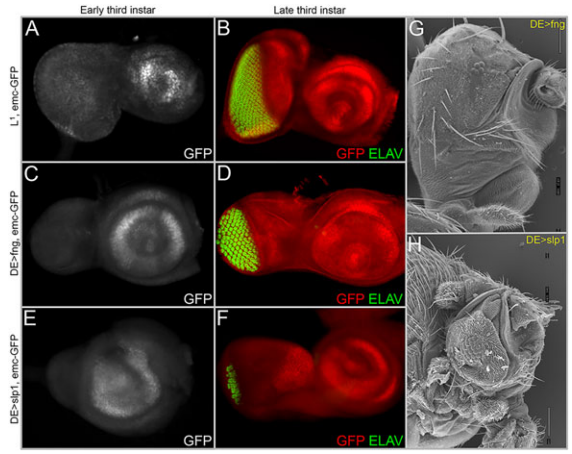

Fig. 2. Disruption of D/V patterning abolishes *emc* midline expression. (A-F) Early third instar (A,C,E) and late third instar (B,D,F) eye imaginal discs. (A,B) In L^1 mutants, which lack a ventral compartment, enrichment of *emc-GFP* along the midline is not detected. Antennal expression of *emc-GFP*, however, is still visible. (C-F) *emc-GFP* enrichment at the midline is lost in discs in which the expression of either *fng* or *slp1* within the dorsal half of the eye has eliminated the dorsal compartment. Again, *emc-GFP* expression is still visible in the antennal compartment. (B,D,F) Expression of *emc-GFP* is also present in the anterior compartment of late third instar discs, but lacks midline enrichment. (G,H) Scanning electron micrographs of *DE>fng* adults and *DE>slp1* pharate adults reveal severe defects in retinal growth that are due to the disruption of D/V patterning. Dorsal side is up and anterior is to the right.

Fig. S1A-G). We also screened five GAL4 strains from the Janelia Farm Research Campus that contained DNA fragments from the *emc* locus and again failed to observe any midline expression (supplementary material Fig. S1A,H-Q). Therefore, the midline enhancer is likely to be located further away than we initially predicted.

We next set out to register the spatial and temporal expression pattern of *emc* with factors involved in D/V patterning and PCP. We first compared *emc* expression with that of *mirr* and *slp1*, which are expressed and function in the dorsal and ventral halves of the eye, respectively (McNeill et al., 1997; Sato and Tomlinson, 2007). The early eye disc lacks a sharp equator and instead has a broad midline region that is ~10-15 cell diameters wide. Whereas neither *mirr* nor *slp1* is expressed within this zone (Sato and Tomlinson, 2007), *emc* is highly enriched within these midline cells (Fig. 1D-I). In addition to *emc*, several genes that function in D/V patterning, such as *Ser*, *Notch* and *fj*, are also expressed within this zone (reviewed by Jenny, 2010). We were particularly interested in *fj* because PCP defects (albeit mild) in the eye are associated with loss-of-function mutant alleles (Zeidler et al., 1999; Strutt et al., 2003). We compared the expression of *emc* and *fj* transcriptional reporters and it appears that the enrichment of *emc* occurs within a large subset of cells that also express *fj* (Fig. 1J-L). The spatial location of *emc* at the midline and its overlapping expression with *fj* suggest a role for Emc in D/V patterning.

emc expression is dependent upon the formation of the midline

We sought to determine whether *emc* expression is dependent upon the establishment of the midline or if Emc itself is required to induce midline formation. To address the first model, we started by analyzing *emc* expression in mutants in which the midline has been abolished. *Lobe* (L^1) mutants are characterized by extensive cell death within the ventral half of the eye, thus leaving only dorsally fated tissue (Chern and Choi, 2002; Singh and Choi, 2003; Singh et al., 2006). In the L^1 mutant eye field, we find that although *emc* is expressed normally within the antenna and ahead of the advancing furrow, the enrichment of *emc* at the midline is entirely lost (Fig. 2A,B). Without the juxtaposition of dorsal and ventral tissue the midline itself probably fails to be specified.

We performed the reciprocal experiment and analyzed *emc* expression in animals with only ventrally fated tissue. This was accomplished by using DE-GAL4 (Morrison and Halder, 2010) to drive expression of the ventral selector genes *fng* and *slp1* in the dorsal half of the eye. Similar to L^1 mutants, *emc* expression along the midline is lost (Fig. 2C-F). In these two cases it is also likely that the midline fails to be specified. Expression of ventral selector genes in the dorsal half of the eye field leads to small and disorganized adult eyes (Fig. 2G,H). The failure to produce a midline is expected to yield small eyes because the midline also serves as the site of Notch- and JAK/STAT-mediated eye growth (Bach et al., 2003; Chao et al., 2004; Tsai and Sun, 2004; Reynolds-Kenneally and Mlodzik, 2005). We also expressed *fng* and *slp1* throughout the eye using an ey-GAL4 driver and in both cases observed that *emc* is no longer enriched at the midline (supplementary material Fig. S2A-F). Curiously, *slp1-lacZ* expression is still restricted to the ventral side of the eye disc despite the use of the ey-GAL4 driver. This might be due to the weak expression of the ey-GAL4 driver or its sometimes patchy and inconsistent expression pattern. We can conclude, however, that in all five genetic backgrounds in which we disrupted normal D/V patterning *emc* enrichment at the midline region of the eye disc is completely abolished (Fig. 2A-F; supplementary material Fig. S2A-F). These results suggest that the juxtaposition of dorsal and ventral tissue is required for *emc* to be expressed along the midline.

Development (2015) 142, 1006-1015 doi:10.1242/dev.120618

We then asked if the creation of artificial D/V boundaries could lead to the ectopic activation of *emc* expression. We used the flp-out system (Struhl and Basler, 1993; Pignoni et al., 1997) to generate clones that overexpress either *mirr* in the ventral compartment or *fng* in the dorsal compartment. These manipulations have been reported to result in the creation of new fng^{+}/fng^{-} boundaries (Cho and Choi, 1998; Dominguez and de Celis, 1998; Papayannopoulos et al., 1998; Sato and Tomlinson, 2007). Echoing wild-type development, the formation of new fng^{+}/fng^{-} boundaries leads to the loss of *mirr*, *fng* and *slp1* and a subsequent elevation of *Ser* expression in a narrow band of cells surrounding the overexpression clones (Sato and Tomlinson, 2007). Since these new D/V boundaries have many hallmarks of the normal midline, we set out to determine whether an enrichment of *emc* expression accompanies the formation of these new boundaries. We were able to confirm this hypothesis as *emc* expression is indeed elevated in the cells bordering the *mirr* and *fng* overexpression clones (Fig. 3A-C,G-I, arrows).

Similar effects were observed when we overexpressed *fng* in the ventral compartment of the wing disc. Compared with the eye, the *fng* expression pattern in the wing is reversed, with *fng* being normally expressed solely within the dorsal compartment (Irvine and Wieschaus, 1994; Kim et al., 1995). When *fng*-expressing clones cross the endogenous D/V border and extend into the ventral compartment, enrichment of *emc* expression is shifted congruently with the formation of a new midline (Fig. 3D-F, arrows).

An additional case in which we can study the effect that the establishment of new fng^{+}/fng^{-} boundaries has on *emc* expression is when *mirr* expression is removed from the dorsal compartment. *fng* expression is ectopically activated in iro^{DFM3} null mutant clones (which are deficient for all three Iro-C genes) that lie within the dorsal half of the eye (Sato and Tomlinson, 2007). The generation of new D/V boundaries by the loss of the Iro-C genes in the dorsal compartment leads to a non-autonomous elevation of *emc* expression in cells surrounding the clone (Fig. 3J-L, arrow). Not all clones within the dorsal compartment show this non-autonomous enrichment within a single disc. We observe an elevation in *emc* expression surrounding the majority of clones and also note that there does not appear to be a domain restriction for this effect – we readily see *emc* upregulation surrounding clones that contact the margin or lie within either the anterior or the posterior compartments. Altogether, we conclude that *emc* expression at the midline, in both the eye and wing, is induced by the juxtaposition of dorsal and ventral compartments.

We next determined whether Emc participates in the establishment of the midline. We generated flp-out overexpression clones of *emc* and analyzed the expression of several genes, including *mirr*, *slp1* and *fj*. As the expression of these genes remains unaltered in *emc* overexpression clones (Fig. 4A-L), we conclude that Emc cannot induce the formation of a D/V boundary. Since Emc loss-of-function mutants have chirality and rotation defects we also examined whether the overexpression of *emc* could induce PCP and rotation defects. We used a transcriptional reporter for *spalt major* (*salm-lacZ*), which is expressed in the R3/4 pair, to visualize rotating photoreceptor clusters (Barrio et al., 1999; Fanto and Mlodzik, 1999; Domingos et al., 2004). Overexpression of *emc* failed to modify the chevron-like pattern of *salm* expression (compare Fig. 4M-P with Fig. 7A,E), suggesting that increased levels of *emc* cannot alter ommatidial chirality and/or rotation.

Notch signaling directs *emc* expression at the D/V midline

The Notch pathway regulates *emc* expression in several developmental contexts, including vein and margin formation in the wing disc, patterning mesodermal segments within the developing embryo, and neural determination in the eye (Baonza et al., 2000; Baonza and Freeman, 2001; Tapanes-Castillo and Baylies, 2004; Bhattacharya and Baker, 2009). In the first two instances, Notch activates the expression of *emc* within the wing and embryo. However, in the developing eye Notch appears to either promote or repress *emc* depending upon the developmental context. Within the morphogenetic furrow *atonal* (*ato*) expression appears to depend upon the repression of *emc* by the Notch pathway (Baonza and Freeman, 2001). By contrast, Notch activation of *emc* transcription is required for R7 and cone cell development (Bhattacharya and Baker, 2009). We sought to determine if Notch signaling regulates *emc* expression at the D/V midline and, if so, whether it is via activation or repression.

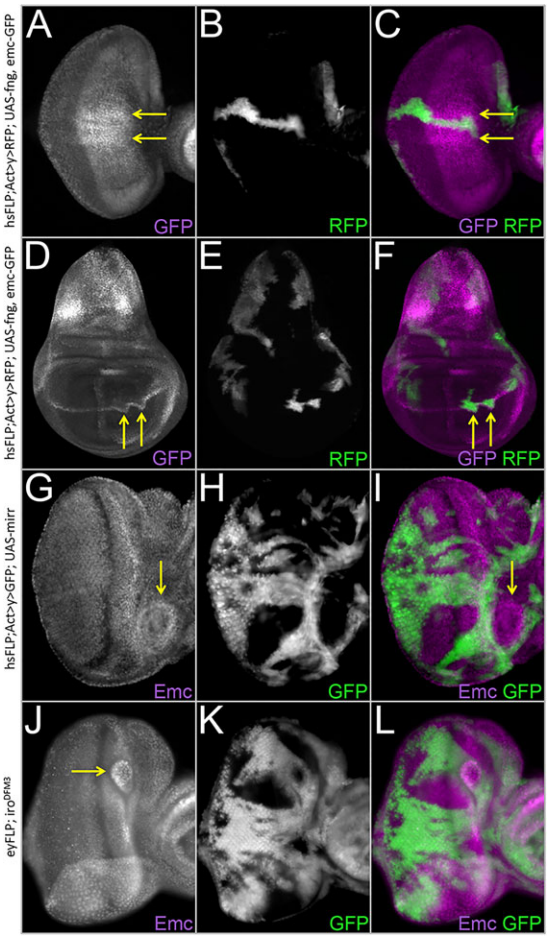

Fig. 3. The induction of new D/V boundaries activates *emc* expression. (A-C) A flp-out clone (*hsFLP/+; Act>y>GFP/+; UAS-fng/emc-GFP*) overexpressing *fng* in the dorsal compartment (RFP-expressing cells in B,C) results in an enrichment of *emc-GFP* at the new fng^{+}/fng^{-} boundary (arrows in A). We also note a decrease in the level of *emc-GFP* within the *fng*-expressing clone. (D-F) In the wing disc, a flp-out clone (same genotype as in A-C) overexpressing *fng* (RFP-expressing cells in E,F) in the ventral compartment shifts the D/V boundary, leading to increased *emc-GFP* expression along the new border (arrows in D, compare with Fig. 5J). (G-I) Flp-out clones (*hsFLP/+; Act>y>GFP/+; UAS-mirr/+*) expressing *mirr* in the ventral compartment (GFP-expressing cells in H,I) have increased Emc protein levels along the new clonal boundaries (arrow in G). (J-L) Loss-of-function clones that are deficient for all three Iro-C genes (*eyFLP/+;* iro^{DFM3}*, FRT80B/Ubi-GFP, FRT80B*) created in the dorsal compartment (lack of GFP in K,L) show an enrichment of Emc antibody staining (arrow in J). Dorsal side is up and anterior is to the right.

Development (2015) 142, 1006-1015 doi:10.1242/dev.120618

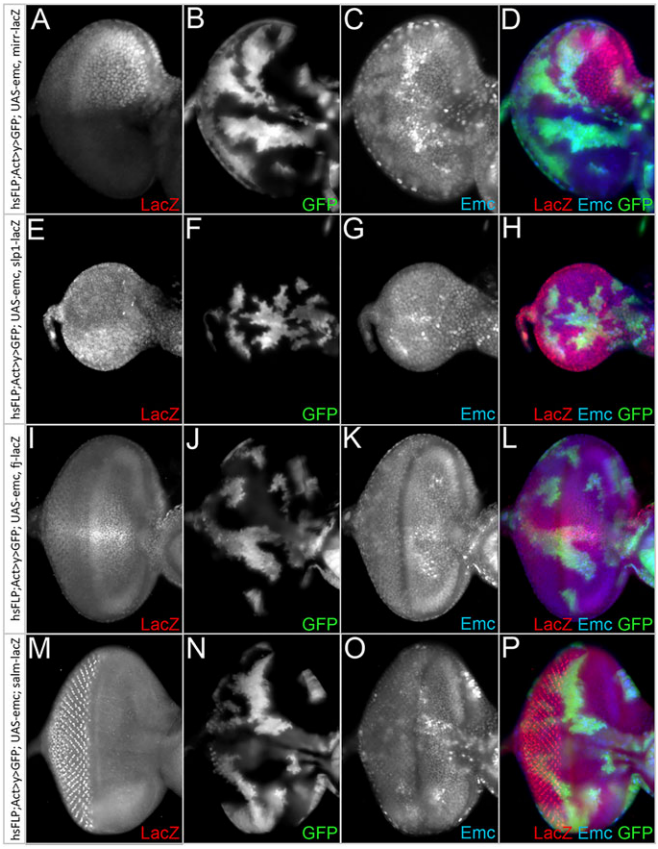

Fig. 4. Expression of *emc* is not sufficient to induce new midlines or alter PCP in the developing eye. (A-D) The overexpression of *emc* (*hsFLP/+; Act>y>GFP/+; mirr-lacZ/UAS-emc*) does not lead to altered *mirr* expression. (E-H) The expression of *slp1* appears normal in *emc* overexpression clones (*hsFLP/+; Act>y>GFP/slp1-lacZ; UAS-emc/+*). (I-L) Flp-out clones overexpressing *emc* do not change *fj* expression (*hsFLP/+; Act>y>GFP/fj-lacZ; UAS-emc/+*). (M-P) PCP and ommatidial rotation marked by the chevron-like orientation of *salm* expression appear normal within *emc* overexpression clones (*hsFLP/+; Act>y>GFP/salm-lacZ; UAS-emc/+*). In all cases, the increased Emc protein level can be visualized (C,G,K,O) within GFP-positive clones (B,F,J,N). Dorsal side is up and anterior is to the right.

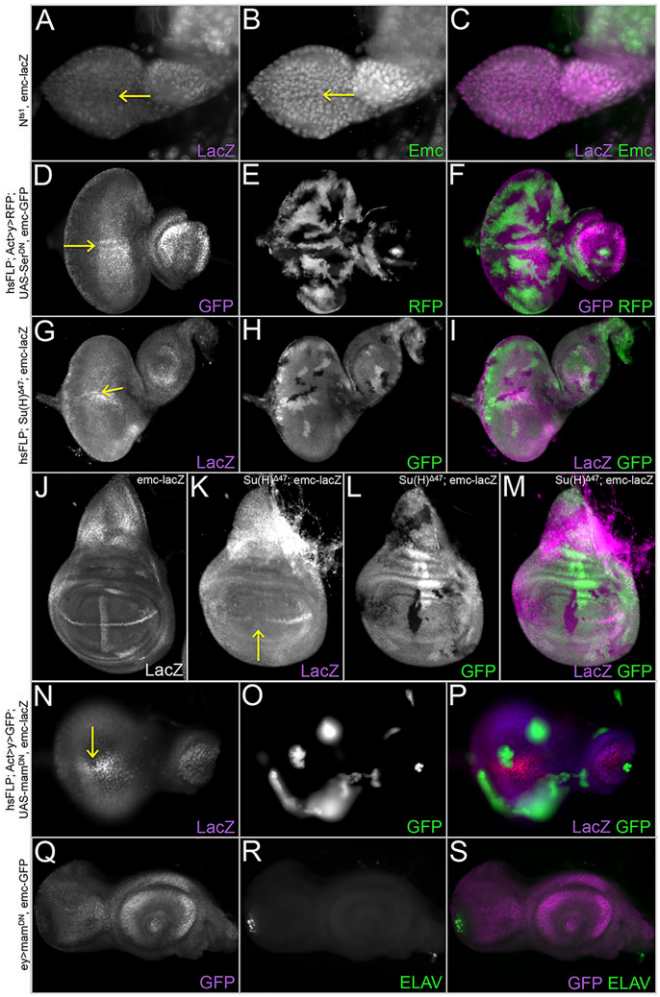

Fig. 5. Notch signaling regulates *emc* expression at the D/V midline in eye and wing discs. (A-C) In N^{ts1} mutants raised at the restrictive temperature, normal enrichment of *emc-GFP* and Emc protein at the midline of the eye is absent (arrows in A,B). Basal levels of *emc* expression are still observed in the eye and antennal discs, indicating that *emc* can be activated independently of Notch signaling. (D-F) A flp-out clone overexpressing a dominant-negative form of *Ser* (Ser^{DN}; GFP-expressing cells in E,F) decreases *emc-lacZ* expression (arrow in D) at the midline. (G-I) Loss-of-function clones of Su(H) (*hsFLP/+; Su(H)$^{\Delta 47}$, FRT40A/Ubi-GFP, FRT40A; emc-lacZ/+*) spanning the midline (lack of GFP in H) display reduced levels of *emc-lacZ* expression (arrow in G). (J) Expression of the *emc-lacZ* reporter in a late third instar wild-type wing disc. Note the enriched expression of *emc-lacZ* along the D/V midline. (K-M) A loss-of-function clone of *Su(H)* (same genotype as G-I) that spans the wing D/V midline (lack of GFP in L,M) shows decreased levels of *emc-lacZ* within the clone (arrow in K). (N-P) Flp-out clones (*hsFLP/+; Act>y>GFP/+; UAS-mam^{DN}/emc-lacZ*) overexpressing a dominant-negative allele of *mam* (cells expressing GFP in O,P) reduce expression of *emc-lacZ* along the midline of the eye (arrow in N). (Q-S) Overexpression of the mam^{DN} allele throughout the eye using ey-GAL4 leads to a loss of *emc* enrichment at the midline. Dorsal side is up and anterior is to the right.

We first increased Notch signaling by expression of its intracellular domain (N^{icd}) in flp-out clones and observed that this manipulation is sufficient to activate an *emc-lacZ* reporter cell-autonomously (supplementary material Fig. S3A-D, arrow). To assess the necessity of the Notch pathway in maintaining *emc* expression we used several different genetic manipulations to reduce the level of Notch activity. First, we used a temperature-sensitive allele of *Notch* (N^{ts1}; Shellenbarger and Mohler, 1975) to block Notch pathway activity and observed that *emc* expression at the midline is specifically eliminated (compare Fig. 1A-C with Fig. 5A-C, arrows), whereas *emc* expression throughout the rest of the eye field appears to be unaffected by the loss of Notch activity. Second, we expressed a dominant-negative allele of *Ser* (Ser^{DN}; Hukriede et al., 1997) as an alternate approach to reducing Notch activity. In flp-out clones expressing Ser^{DN} we also observed downregulation of *emc* expression at the midline (Fig. 5D-F, arrow). Third, we removed Notch activity by inducing clones of a *Su(H)* loss-of-function mutant allele and again observed that *emc* expression along the midline within the eye and wing is lost (Fig. 5G-M, arrow). Lastly, we generated flp-out overexpression clones of a dominant-negative form of *mastermind* (mam^{DN}), which encodes a co-factor for Su(H) (Helms et al., 1999). In this case, as with all the others, *emc* expression is lost when mam^{DN} is expressed either in clones (Fig. 5N-P, arrow) or throughout the entire eye field (Fig. 5Q-S). Su(H) and Mam are DNA-binding proteins and therefore the pattern of *emc* loss is informative: reduction in both proteins leads to the cell-autonomous loss of *emc* expression and this supports the contention that the Notch pathway directly regulates *emc* transcription. These findings are also consistent with the cell-autonomous activation of *emc* in N^{icd} overexpression clones

Development (2015) 142, 1006-1015 doi:10.1242/dev.120618

(supplementary material Fig. S3A-D). The Notch pathway is required not only at the midline, as clones that include non-midline tissue in the wing also show reductions in *emc* expression (Fig. 5J-M).

The Notch pathway bifurcates downstream of Su(H), with genes of the Enhancer of split complex [E(spl)-C] residing within one branch (de Celis et al., 1996). The forced expression of several E(spl)-C genes (*mβ*, *m5* and *m8*) does not affect *emc* expression (supplementary material Fig. S4A-L), suggesting that *emc* lies within a separate branch of the cascade. Overall, our results support a model in which an E(Spl)-independent branch of the Notch pathway directly activates *emc* expression at the D/V boundary within developing eye and wing discs.

Emc functions downstream of Notch signaling to regulate *fj*

fj is expressed in a gradient within the eye disc, with the highest levels at the midline (Fig. 1J) (Brodsky and Steller, 1996; Strutt et al., 2003). Similarly, in the wing disc *fj* is expressed at the highest level within central regions of the pouch and at lower levels in peripheral regions (Fig. 6D) (Strutt et al., 2003). The Notch pathway has been proposed to directly regulate *fj* expression in both tissues (Zeidler et al., 1999). However, the conspicuous overlap of *fj* and *emc* expression at the midline in the eye and wing, as well as the requirement for Notch signaling in maintaining *emc* expression, prompted us to test a model in which Notch regulation of *fj* requires Emc activity. We generated emc^{AP6} null clones in the eye and wing and analyzed the expression of a *fj-lacZ* reporter. In both tissues, we observe a cell-autonomous reduction in *fj* expression (Fig. 6A-C,F,G, arrow). *fj-lacZ* expression is not completely eliminated in *emc* mutant tissue, which is consistent with previous findings that additional signals from the JAK/STAT and Wg pathways also regulate *fj* expression at the midline (Zeidler et al., 1999; Gutierrez-Aviño et al., 2009). To determine if JAK/STAT regulation of *fj* is also through Emc we analyzed *emc* expression in both *Stat92E* overexpression (supplementary material Fig. S5A-C) and loss-of-function (supplementary material Fig. S5D-F) clones. In both cases, we see no effect on *emc* expression and therefore conclude that Notch activates *fj* expression via *emc*, while JAK/STAT signaling has a separate input into *fj*.

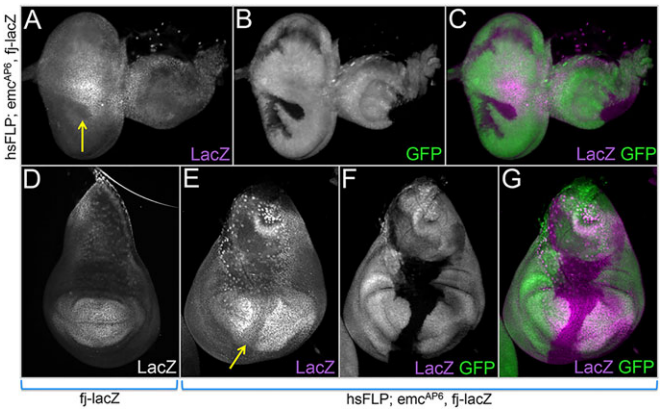

Fig. 6. *fj* expression is dependent upon the activity of Emc in the developing eye and wing. (A-C) In the eye disc, clones null for *emc* (*hsFLP/+; fj-lacZ/+; emc^{AP6}, FRT80B/Ubi-GFP, FRT80B M(3)^{i55}*; GFP-negative cells in B,C) have decreased expression of *fj-lacZ* (arrow in A). (D) Wild-type *fj-lacZ* reporter expression within wing disc (E-G) *emc* null clones (same genotype as A-C; lack of GFP in F,G) in the wing pouch also show decreased expression of *fj* (arrow in E). In both types of discs we note an accumulation of *fj-lacZ* expression along the clonal boundary of these clones. Dorsal side is up and anterior is to the right.

Emc is required for proper PCP and ommatidial rotation

The PCP defects seen in clones of the emc^{1} hypomorphic allele are very mild (Brown et al., 1995) and probably do not reveal the full role that Emc plays in either ommatidial rotation or PCP. We generated and analyzed both types of defects in emc^{AP6} null mutant clones. On their own, emc^{AP6} mutant cells proliferate very slowly and thus the clones are very small and difficult to analyze. To overcome this obstacle we provided the emc^{AP6} cells with a growth advantage by generating the clones in a *Minute* ($M3^{i55}$) heterozygous mutant background. When placed against $M(3)^{i55}$/+ heterozygous tissue the emc^{AP6} null mutant clones are large and can be analyzed for both rotation and PCP defects in the imaginal disc and in adult retinal sections. In emc^{AP6} clones, the majority of ommatidia have properly specified R3/4 pairs but the chevron-like arrangement is substantially disrupted (Fig. 7A-F), suggesting that ommatidial rotation has not been completed properly. In Fig. 7F it is possible to see ommatidia that have not rotated correctly (green arrows).

In order to determine whether chirality is also affected, we looked at the orientation of ommatidia in adult retinal sections. In a normally constructed ommatidium, the rhabdomeres of the R1-7 photoreceptors are arranged in an asymmetrical trapezoid (Fig. 7G) (Dietrich, 1909; Chen, 1929; Waddington and Perry, 1960). The trapezoids of the dorsal and ventral compartments are arranged as mirror images of each other with the two chiral forms meeting at the equator (Ready et al., 1976). Within *emc* null clones a significant number of ommatidia have either fewer than the normal number of photoreceptors (Fig. 7H,I, red circles) or have undergone significant degeneration (Fig. 7H,I, blue circles). In both cases we were unable to determine the chirality of the ommatidia. However, in several instances we were able to clearly see ommatidia with inappropriate chirality (Fig. 7H,I, purple arrow) or ommatidia in which both the R3 and R4 precursor cells have adopted the R3 fate (Fig. 7H,I, red arrows). By far the most common defect in the adult retina is the incorrect rotation of ommatidia (Fig. 7H,I, green arrows), which also seemed to be the predominant phenotype in the developing eye disc (Fig. 7F). Since so many ommatidia could not be scored for either chirality or rotation, our analysis most likely underestimates the role that Emc plays in PCP and rotation.

As *fj* loss-of-function mutants have mild chirality defects and no rotation defects we investigated whether *emc* regulates the Ft/Ds system. In *emc* loss-of-function clones, *ds* expression levels (using a *ds-lacZ* reporter) appear relatively normal (supplementary material Fig. S6A-H), suggesting that Emc influences PCP by regulating other factors outside of the Ft/Ds system. Since *wg* expression is reduced in *emc* clones that contact the margin (Spratford and Kumar, 2013), it is possible that the PCP and rotation defects that are seen in *emc* mutant tissue are in part due to the regulation of Wg signaling.

DISCUSSION

Two prior studies have indicated that Emc is a key player in patterning the D/V axis of the developing *Drosophila* eye. Both reports provide evidence that ommatidia lacking *emc* have a propensity to adopt the incorrect chiral form and fail to rotate properly (Brown et al., 1995; Bhattacharya and Baker, 2009). However, the mechanism by which Emc exerts controls over D/V patterning has not been elucidated. The latter report did suggest that Emc does not function within the R3/4 photoreceptor pair to

Development (2015) 142, 1006-1015 doi:10.1242/dev.120618

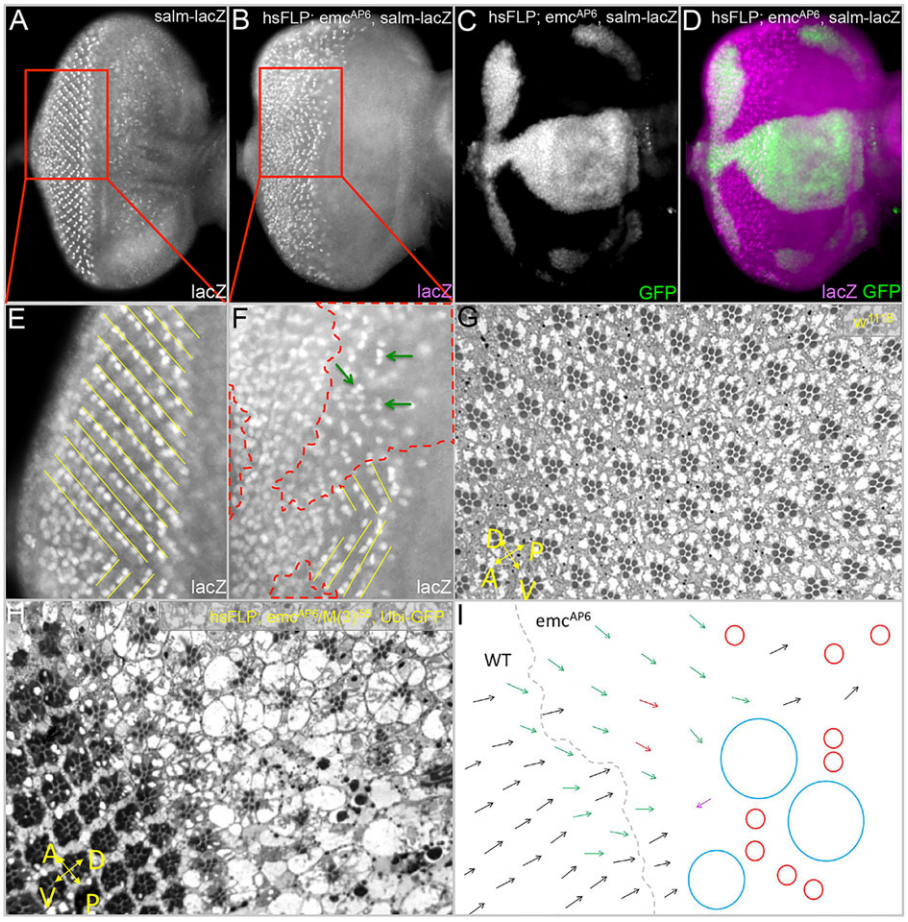

Fig. 7. Emc is required for normal PCP and ommatidial rotation within the developing eye. (A) Third instar eye imaginal disc expressing the *salm-lacZ* reporter. (E) An enlargement of the boxed area in A displaying *salm-lacZ* expression in R3/4 cells. Yellow lines emphasize the mirror image rotation that ommatidia in the dorsal and ventral halves of the eye undergo. (B-D) *emc* loss-of-function clones (*hsFLP/+; salm-lacZ/+; emc^{AP6}, FRT80B/Ubi-GFP, M(3)^{i55}, FRT80B*) show a disrupted pattern of *salm-lacZ* expression. (F) An enlargement of the boxed area in B shows the disruption of *salm-lacZ* expression and the incorrect orientation of ommatidia. Red dashed lines demarcate the clonal boundary. Yellow lines indicate properly rotating ommatidia within the surrounding wild-type tissue. (G) Section of an adult wild-type retina showing normal chirality and ommatidial organization. (H) Section of an adult retina containing an *emc* null clone (*hsFLP; emc^{AP6}, FRT80B/Ubi-GFP, M(3)^{i55}, FRT80B*). (I) A graphic representation of the chirality and rotation of ommatidia in H. The gray dashed line signifies the boundary between *emc* null and wild-type tissue. Black arrows depict ommatidia with seven distinct rhabdomeres with proper structure, chirality and rotation. Green arrows represent ommatidia with correct structure that have incorrectly rotated. Red arrows denote ommatidia that appear to have two R3 cells and thus cannot be scored for chirality. The purple arrow marks an ommatidium that has incorrect chirality. Red circles show ommatidia with fewer than seven rhabdomeres that cannot be scored for chirality. Blue circles signify large areas of the retina devoid of obvious photoreceptor clusters. The orientation of the retina is marked in G and H. For other panels dorsal side is up and anterior is to the right.

promote PCP. These cells use the Fz and Notch pathways to receive and amplify a polarizing signal (Zheng et al., 1995; Cooper and Bray, 1999; Fanto and Mlodzik, 1999; Tomlinson and Struhl, 1999). In *emc* mutant tissue the vast majority of R4 cells are properly specified and Notch signaling, as assayed by an E(spl)mδ reporter, appears normal (Bhattacharya and Baker, 2009). Thus, it is unlikely that *emc*, although expressed in the R3/4 neurons, functions in these cells to promote ommatidial chirality and rotation (Bhattacharya and Baker, 2009).

The other sites within the developing eye at which Emc could function to promote PCP are the margins where Wg and Ds levels are highest and at the D/V midline where *fj* expression is enriched (Fig. 8A,B). We have previously shown that in young eye discs *emc* expression is distinctly enriched at the midline (Spratford and Kumar, 2013). This enrichment persists in the anterior compartment in older discs (Brown et al., 1995; Bhattacharya and Baker, 2009; Spratford and Kumar, 2013); therefore, Emc may regulate *fj* expression at the midline. In that same study we also demonstrated that Wg expression at the ventral margin depends on *emc* expression (Fig. 8B) (Spratford and Kumar, 2013) and therefore Emc could, in principle, also regulate Ds protein levels.

In this study we set out to determine the mechanism by which Emc functions in D/V patterning. We first refined our analysis of *emc* transcription and showed that *emc* is enriched within a zone of cells at the midline that lies between the expression domains of the dorsal selector gene *mirr* and the ventral compartment gene *slp1* (Fig. 1A-I). The expression of *emc* at the midline appears to be dependent upon the juxtaposition of dorsal and ventral fated tissue. When we generate an entire field made up of a single compartment (either dorsal or ventral), enrichment of midline *emc* expression is lost (Fig. 2A-F; supplementary material Fig. S2A-F), and if we induce new D/V boundaries *emc* expression is ectopically induced at the new midline (Fig. 3J-L). It appears that Emc does not play a role in establishing the midline, as ectopic expression of *emc* is insufficient to induce ectopic D/V borders (Fig. 4A-P).

Development (2015) 142, 1006-1015 doi:10.1242/dev.120618

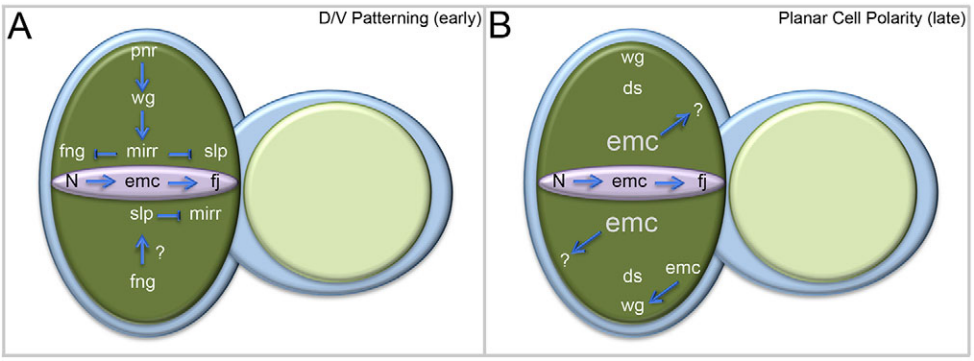

Fig. 8. Emc influences early D/V patterning and PCP in the developing *Drosophila* eye. (A) Emc expression is activated at the midline by the juxtaposition of dorsal and ventral compartments. At the D/V midline, *emc* lies downstream of the Su(H)-Mam complex to activate the expression of *fj*. (B) In mid/late third instar discs, Emc regulates the expression of *wg* along the ventral margin and *fj* at the midline. Since *emc* is expressed throughout the disc it might influence PCP and rotation via additional targets. Our data suggest that *ds* is not one such target, as its expression appears relatively normal in *emc* mutant clones. Dorsal side is up and anterior is to the right.

How is *emc* expression activated at the midline in response to the juxtaposition of fng^{+} and fng^{-} cells? The confrontation of these two populations of cells leads to the activation of Notch signaling at the midline. Emc has been placed downstream of the Notch pathway in several developmental contexts, including developing photoreceptors and the wing. Here, we have determined that Notch signaling promotes *emc* expression at the midline via the Su(H)-Mam complex (Fig. 5, Fig. 8A,B; supplementary material Fig. S3A-D). What is the function of Emc at the midline? Prior reports had suggested that N signaling activates *fj* expression directly via Su(H) (Zeidler et al., 1999; Gutierrez-Aviño et al., 2009). Since *emc* expression overlaps significantly with *fj* at the midline (Fig. 1J-L), we tested the validity of an alternative model in which Notch activation of *emc* is required to regulate *fj* expression. We provide evidence that *emc* functions to maintain *fj* expression at the midline – *fj* expression is greatly reduced in *emc* loss-of-function clones (Fig. 6A-G, Fig. 8A,B). Also, as expression of *emc* is unable to induce *fj* expression it is more likely that Emc is instead required to maintain *fj* expression. Since *fj* plays a minor role in PCP within the eye, only a fraction of the chirality defects seen in *emc* mutant tissue are likely to be caused by the loss of *fj*. The majority of chirality defects and all of the rotation defects that are seen in *emc* mutants (Fig. 7) (Brown et al., 1995; Bhattacharya and Baker, 2009) are likely to be due to dysregulation of Wg signaling and other factors.

Four *emc* homologs encoded within the vertebrate genome are referred to as the inhibitor of DNA binding genes (*Id1-4*) (Benezra et al., 1990; Christy et al., 1991; Sun et al., 1991; Biggs et al., 1992; Ellmeier et al., 1992; Deed et al., 1993; Riechmann et al., 1994; Zhu et al., 1995). To date, a role for the Id proteins in D/V patterning of the vertebrate retina has not been reported. This might be a result of functional redundancy. All Id proteins are expressed within the retina and several are transcribed early in development. For example, within the mouse retina *Id1-3* are expressed early in the optic vesicle and the overlying surface ectoderm, then later in the ganglion and neuroblastic layers of the optic cup, with expression persisting in the retinal ganglion cells and in both rod and cone photoreceptors (Ellmeier and Weith, 1995; Jen et al., 1996, 1997; Yeung and Yip, 2005; Du and Yip, 2011). By contrast, *Id4* expression is restricted to the neural layer of the optic cup (Jen et al., 1996). It has been proposed that, like the fly retina, the vertebrate eye might also be born with just ventral identity and that dorsal fates are imposed later in development (Murali et al., 2005). This model is of particular interest, as one or more Id proteins might play a role similar to that of Emc in regulating D/V patterning in the vertebrate retina. It is intriguing to think that roles for Emc/Id in D/V patterning might not be limited to the retina. Manipulations of vertebrate PCP genes lead to developmental defects within the mammalian kidney (reviewed by Carroll and Yu, 2012). Id1-3 are expressed within the developing mouse kidney and in rat cultured kidney glomerular mesangial cells (Jen et al., 1996). If Emc/Id proteins are shown to play a conserved role in D/V patterning then considerable light might soon be shed on mammalian development and disease.

MATERIALS AND METHODS

Fly stocks

(1) *emc-GFP^{YB0067}/TM3*; (2) *P{PZ}emc^{04322}/TM3*; (3) *w^{1118}*; (4) *w*; mirr^{B1-12}/TM6B*; (5) *P{PZ}slp1^{05965}/CyO*; (6) *fj-lacZI*; (7) *L^{1}*; (8) *eyFLP; DE-GAL4/TM6B*; (9) *UAS-fng, emc-GFP^{YB0067}/TM3*; (10) *y^{1} w*; UAS-slp1/CyO*; (11) *hsFLP^{22}*; (12) *Act5C>y+>Gal4, UAS-RFP/TM3*; (13) *Act5C>y+>GAL4, UAS-GFP*; (14) *UAS-mirr*; (15) *y^{1} w* eyFLP*; (16) *y^{1} w* hsFLP; iro^{DFM3} FRT2A/TM3*; (17) *Ubi-GFP FRT80B*; (18) *y^{1} N^{ts1} g^{2} f^{1}/C(1)DX y^{1} f^{1}*; (19) *UAS-Ser^{DN}, emc-GFP^{YB0067}/TM6*; (20) *Su(H)$^{\Delta 47}$ FRT40A [w+l(2)35Bg+]/CyO*; (21) *w^{1118}; Ubi-GFPnls FRT40A/CyO*; (22) *UAS-mam^{DN}*; (23) *y^{1} w* hsFLP^{22}; emc^{AP6} FRT80B/TM6B*; (24) *y^{1} w* hsFLP^{22}; Ubi-GFP M(3)^{i55} FRT80B/TM6B*; (25) *UAS-emc4M*; (26) *P{PZ} salm^{03602}/CyO*; (27) *emc-E1-lacZ*; (28) *emc-E2-lacZ*; (29) *emc-E3-lacZ/TM3*; (30) *GMR10D04-GAL4*; (31) *GMR10H11-GAL4*; (32) *GMR10B05-GAL4*; (33) *GMR10C04-GAL4*; (34) *GMR10B08-GAL4*; (35) *UAS-lacZ*; (36) *UAS-Stat92E*; (37) *w*; FRT82B Stat92E^{85c9}/TM6B*; (38) *FRT82B Ubi-GFPnls*; (39) *y^{1} w* M{vas-int.Dm}ZH-2A; PBac{y+-attP-3B} VK00033*; (40) *y^{1} v^{1}; P{TRiP.JF02100} attP2/TM3*; (41) *y^{1} w*; UAS-E(spl)mβ$^{48.1}$*; (42) *UAS-E(spl)m8*; (43) *UAS-E(spl)m5*; (44) *UAS-N^{icd}*; (45) *salm-lacZ*; (46) *ey-GAL4*. Stocks 1-7, 11-18, 20, 21, 26, 30-35, 38-43, 45 and 46 were from the Bloomington Drosophila Stock Center; stock 8 is from Georg Halder (VIB Vesalius Research Center, KU Leuven, Belgium); stock 9 is a combination of two stocks from the Bloomington Drosophila Stock Center; stock 10 is from Andrew Tomlinson (Columbia University, NY, USA); stock 19 is a combination of *UAS-Ser^{DN}* from Robert Fleming (Trinity College, Hartford, CN, USA) and *emc-GFP^{YB0067}* from the Bloomington Drosophila Stock Center; stock 22 is from Barry Yedvobnick (Emory University, Atlanta, GA, USA); stocks 23 and 24 are from Nick Baker (Albert Einstein College of Medicine, NY, USA; stock 25 is from Antonio Baonza (Centro de Biología Molecular Severo Ochoa (CSIC/UAM), Madrid, Spain); stocks 27-29 were generated by C.M.S.; stocks 36 and 37 are from Erika Bach (New York University, USA); stock 44 is from Kevin Moses (Wellcome Trust, London, UK).

Antibodies and microscopy

Primary antibodies: rat anti-Elav (1:100; Developmental Studies Hybridoma Bank); rabbit anti-Emc (1:1000; Yuh Nung Jan, UCSF, CA, USA); and

Development (2015) 142, 1006-1015 doi:10.1242/dev.120618

mouse anti-β-gal (1:100; Promega, Z3781). Flurophore-conjugated secondary antibodies and phalloidin-flurophore conjugates were obtained from Jackson Laboratories and Molecular Probes. Imaginal discs were prepared as described by Anderson et al. (2012). Immunostaining was carried out according to Spratford and Kumar (2014). For scanning electron microscopy, adults or pharate adults were serially incubated in 25% ethanol, 50% ethanol, 75% ethanol, 100% ethanol, 50% ethanol:50% hexamethyldisilazane (HMDS) and 100% HMDS, coated with gold-palladium and viewed with a JEOL 5800LV scanning electron microscope. Retinal sections were prepared as described by Jenny (2010). Slides were photographed on a Zeiss Axioplan II compound microscope.

Temperature shift regimes

For *Notch* temperature-sensitive mutants, an *emc-lacZ* reporter was crossed to the N^{ts1} strain and flies were allowed to lay eggs in vials at 25°C for 48 h. Adults were transferred to new vials, following which the old vial was incubated at 16°C for 24-96 h. Once first instar larvae were visible, vials were moved to the restrictive temperature of 30°C for 24-48 h before dissection of early third instar larvae. All heat shock-induced clones were induced at 37°C 48 h after egg lay. emc^{AP6} loss-of-function clones were induced by a 20 min heat pulse followed by a 60 min rest period (at room temperature) and a second 20 min heat pulse. Overexpression and MARCM clones were induced with 20 min and 60 min heat pulses, respectively. At least ten discs containing clones were analyzed for each genotype. Each phenotype documented within figures was observed in at least 50% of clones.

Cloning and analysis of *emc* enhancers

The three putative enhancer regions illustrated in supplementary material Fig. S1 were amplified from w^{1118} genomic DNA by PCR and cloned into the placZ.attB plasmid (Konrad Basler, University of Zurich, Switzerland). Cloning strategies and PCR conditions are described in the supplementary Methods; for primers see supplementary material Table S1. The p.enhancer. lacZ.attB constructs were transformed into flies and stable stocks were created and analyzed for *lacZ* expression in imaginal and brain tissue.

Acknowledgements

We thank Brandon Weasner and Bonnie Weasner for technical support with the cloning of enhancer constructs and the generation of transgenic fly strains; Rudi Turner for generating retinal sections and scanning electron micrographs of adult eyes; Konrad Basler, Andrew Tomlinson, Yuh-Nung Jan, Nick Baker, Alan Spradling, Lynn Cooley, Antonio Baonza Erika Bach, Robert Fleming, Georg Halder, Kevin Moses, Barry Yedvobnick and the Bloomington Drosophila Stock Center for DNA plasmids, antibodies and fly stocks; and Utpal Banerjee for generously allowing C.M.S. to complete a portion of this work in his lab.

Competing interests

The authors declare no competing or financial interests.

Author contributions

C.M.S. and J.P.K. designed experiments, analyzed data and wrote the manuscript. C.M.S. carried out the experiments and collected the data.

Funding

This work was supported by a stipend from the National Institutes of Health (NIH) GCMS Training Grant [T32-GM007757], a Frank W. Putnam Research Fellowship and a Robert Briggs Research Fellowship to C.M.S. and a grant from the National Eye Institute [R01 EY014863] to J.P.K. Deposited in PMC for release after 12 months.

Supplementary material

Supplementary material available online at
http://dev.biologists.org/lookup/suppl/doi:10.1242/dev.120618/-/DC1

References

Alifragis, P., Poortinga, G., Parkhurst, S. M. and Delidakis, C. (1997). A network of interacting transcriptional regulators involved in Drosophila neural fate specification revealed by the yeast two-hybrid system. *Proc. Natl. Acad. Sci. USA* **94**, 13099-13104.

Anderson, A. M., Weasner, B. M., Weasner, B. P. and Kumar, J. P. (2012). Dual transcriptional activities of SIX proteins define their roles in normal and ectopic eye development. *Development* **139**, 991-1000.

Ayukawa, T., Akiyama, M., Mummery-Widmer, J. L., Stoeger, T., Sasaki, J., Knoblich, J. A., Senoo, H., Sasaki, T. and Yamazaki, M. (2014). Dachsous-dependent asymmetric localization of spiny-legs determines planar cell polarity orientation in Drosophila. *Cell Rep.* **8**, 610-621.

Bach, E. A., Vincent, S., Zeidler, M. P. and Perrimon, N. (2003). A sensitized genetic screen to identify novel regulators and components of the Drosophila janus kinase/signal transducer and activator of transcription pathway. *Genetics* **165**, 1149-1166.

Baonza, A. and Freeman, M. (2001). Notch signalling and the initiation of neural development in the Drosophila eye. *Development* **128**, 3889-3898.

Baonza, A., de Celis, J. F. and Garcia-Bellido, A. (2000). Relationships between extramacrochaetae and Notch signalling in Drosophila wing development. *Development* **127**, 2383-2393.

Barrio, R., de Celis, J. F., Bolshakov, S. and Kafatos, F. C. (1999). Identification of regulatory regions driving the expression of the Drosophila spalt complex at different developmental stages. *Dev. Biol.* **215**, 33-47.

Benezra, R., Davis, R. L., Lockshon, D., Turner, D. L. and Weintraub, H. (1990). The protein Id: a negative regulator of helix-loop-helix DNA binding proteins. *Cell* **61**, 49-59.

Bhattacharya, A. and Baker, N. E. (2009). The HLH protein Extramacrochaetae is required for R7 cell and cone cell fates in the Drosophila eye. *Dev. Biol.* **327**, 288-300.

Biggs, J., Murphy, E. V. and Israel, M. A. (1992). A human Id-like helix-loop-helix protein expressed during early development. *Proc. Natl. Acad. Sci. USA* **89**, 1512-1516.

Bohn, H. (1967). Transplantation experiments mit interkalarer regeneration zum Nachweis eines sich segmental wiederholenden Gradienten in Beim von Leucophaea (Blattaria). *Zool. Anz. (Supp)* **30**, 499-508.

Brittle, A., Thomas, C. and Strutt, D. (2012). Planar polarity specification through asymmetric subcellular localization of Fat and Dachsous. *Curr. Biol.* **22**, 907-914.

Brodsky, M. H. and Steller, H. (1996). Positional information along the dorsal-ventral axis of the Drosophila eye: graded expression of the four-jointed gene. *Dev. Biol.* **173**, 428-446.

Brown, N. L., Sattler, C. A., Paddock, S. W. and Carroll, S. B. (1995). Hairy and emc negatively regulate morphogenetic furrow progression in the Drosophila eye. *Cell* **80**, 879-887.

Bryant, P. J. (1970). Cell lineage relationships in the imaginal wing disc of Drosophila melanogaster. *Dev. Biol.* **22**, 389-411.

Carroll, T. J. and Yu, J. (2012). The kidney and planar cell polarity. *Curr. Top. Dev. Biol.* **101**, 185-212.

Cavodeassi, F., Diez del Corral, R., Campuzano, S. and Dominguez, M. (1999). Compartments and organising boundaries in the Drosophila eye: the role of the homeodomain Iroquois proteins. *Development* **126**, 4933-4942.

Chao, J.-L., Tsai, Y.-C., Chiu, S.-J. and Sun, Y. H. (2004). Localized Notch signal acts through eyg and upd to promote global growth in Drosophila eye. *Development* **131**, 3839-3847.

Chen, T.-Y. (1929). On the development of imaginal buds in normal and mutant Drosophila melanogaster. *J. Morphol.* **47**, 135-199.

Chern, J. J. and Choi, K. W. (2002). Lobe mediates Notch signaling to control domain-specific growth in the Drosophila eye disc. *Development* **129**, 4005-4013.

Cho, K.-O. and Choi, K.-W. (1998). Fringe is essential for mirror symmetry and morphogenesis in the Drosophila eye. *Nature* **396**, 272-276.

Choi, K.-W. and Benzer, S. (1994). Rotation of photoreceptor clusters in the developing Drosophila eye requires the nemo gene. *Cell* **78**, 125-136.

Christy, B. A., Sanders, L. K., Lau, L. F., Copeland, N. G., Jenkins, N. A. and Nathans, D. (1991). An Id-related helix-loop-helix protein encoded by a growth factor-inducible gene. *Proc. Natl. Acad. Sci. USA* **88**, 1815-1819.

Clark, H. F., Brentrup, D., Schneitz, K., Bieber, A., Goodman, C. and Noll, M. (1995). Dachsous encodes a member of the cadherin superfamily that controls imaginal disc morphogenesis in Drosophila. *Genes Dev.* **9**, 1530-1542.

Cooper, M. T. D. and Bray, S. J. (1999). Frizzled regulation of Notch signalling polarizes cell fate in the Drosophila eye. *Nature* **397**, 526-530.

de Celis, J. F., de Celis, J., Ligoxygakis, P., Preiss, A., Delidakis, C. and Bray, S. (1996). Functional relationships between Notch, Su(H) and the bHLH genes of the E(spl) complex: the E(spl) genes mediate only a subset of Notch activities during imaginal development. *Development* **122**, 2719-2728.

Deed, R. W., Bianchi, S. M., Atherton, G. T., Johnston, D., Santibanez-Koref, M., Murphy, J. J. and Norton, J. D. (1993). An immediate early human gene encodes an Id-like helix-loop-helix protein and is regulated by protein kinase C activation in diverse cell types. *Oncogene* **8**, 599-607.

Dietrich, W. (1909). Die Fazettenaugen der Dipteren. *Z. Wiss. Zool.* **92**, 465-539.

Domingos, P. M., Mlodzik, M., Mendes, C. S., Brown, S., Steller, H. and Mollereau, B. (2004). Spalt transcription factors are required for R3/R4 specification and establishment of planar cell polarity in the Drosophila eye. *Development* **131**, 5695-5702.

Dominguez, M. and de Celis, J. F. (1998). A dorsal/ventral boundary established by Notch controls growth and polarity in the Drosophila eye. *Nature* **396**, 276-278.

Du, Y. and Yip, H. K. (2011). The expression and roles of inhibitor of DNA binding helix-loop-helix proteins in the developing and adult mouse retina. *Neuroscience* **175**, 367-379.

Ellis, H. M., Spann, D. R. and Posakony, J. W. (1990). extramacrochaetae, a negative regulator of sensory organ development in Drosophila, defines a new class of helix-loop-helix proteins. *Cell* **61**, 27-38.
Ellmeier, W. and Weith, A. (1995). Expression of the helix-loop-helix gene Id3 during murine embryonic development. *Dev. Dyn.* **203**, 163-173.
Ellmeier, W., Aguzzi, A., Kleiner, E., Kurzbauer, R. and Weith, A. (1992). Mutually exclusive expression of a helix-loop-helix gene and N-myc in human neuroblastomas and in normal development. *EMBO J.* **11**, 2563-2571.
Fanto, M. and Mlodzik, M. (1999). Asymmetric Notch activation specifies photoreceptors R3 and R4 and planar polarity in the Drosophila eye. *Nature* **397**, 523-526.
Garcia-Bellido, A. and Merriam, J. R. (1971a). Genetic analysis of cell heredity in imaginal discs of Drosophila melanogaster. *Proc. Natl. Acad. Sci. USA* **68**, 2222-2226.
Garcia-Bellido, A. and Merriam, J. R. (1971b). Parameters of the wing imaginal disc development of Drosophila melanogaster. *Dev. Biol.* **24**, 61-87.
Garrell, J. and Modolell, J. (1990). The Drosophila extramacrochaetae locus, an antagonist of proneural genes that, like these genes, encodes a helix-loop-helix protein. *Cell* **61**, 39-48.
Gutierrez-Aviño, F. J., Ferres-Marco, D. and Dominguez, M. (2009). The position and function of the Notch-mediated eye growth organizer: the roles of JAK/STAT and four-jointed. *EMBO Rep.* **10**, 1051-1058.
Heberlein, U., Borod, E. R. and Chanut, F. A. (1998). Dorsoventral patterning in the Drosophila retina by wingless. *Development* **125**, 567-577.
Heitzler, P., Haenlin, M., Ramain, P., Calleja, M. and Simpson, P. (1996). A genetic analysis of pannier, a gene necessary for viability of dorsal tissues and bristle positioning in Drosophila. *Genetics* **143**, 1271-1286.
Helms, W., Lee, H., Ammerman, M., Parks, A. L., Muskavitch, M. A. T. and Yedvobnick, B. (1999). Engineered truncations in the Drosophila mastermind protein disrupt Notch pathway function. *Dev. Biol.* **215**, 358-374.
Hukriede, N. A., Gu, Y. and Fleming, R. J. (1997). A dominant-negative form of Serrate acts as a general antagonist of Notch activation. *Development* **124**, 3427-3437.
Irvine, K. D. and Wieschaus, E. (1994). fringe, a boundary-specific signaling molecule, mediates interactions between dorsal and ventral cells during Drosophila wing development. *Cell* **79**, 595-606.
Ishikawa, H. O., Takeuchi, H., Haltiwanger, R. S. and Irvine, K. D. (2008). Four-jointed is a Golgi kinase that phosphorylates a subset of cadherin domains. *Science* **321**, 401-404.
Jen, Y., Manova, K. and Benezra, R. (1996). Expression patterns of Id1, Id2, and Id3 are highly related but distinct from that of Id4 during mouse embryogenesis. *Dev. Dyn.* **207**, 235-252.
Jen, Y., Manova, K. and Benezra, R. (1997). Each member of the Id gene family exhibits a unique expression pattern in mouse gastrulation and neurogenesis. *Dev. Dyn.* **208**, 92-106.
Jenny, A. (2010). Planar cell polarity signaling in the Drosophila eye. *Curr. Top. Dev. Biol.* **93**, 189-227.
Kim, J., Irvine, K. D. and Carroll, S. B. (1995). Cell recognition, signal induction, and symmetrical gene activation at the dorsal-ventral boundary of the developing Drosophila wing. *Cell* **82**, 795-802.
Lawrence, P. A. and Morata, G. (1976). Compartments in the wing of Drosophila: a study of the engrailed gene. *Dev. Biol.* **50**, 321-337.
Mahoney, P. A., Weber, U., Onofrechuk, P., Biessmann, H., Bryant, P. J. and Goodman, C. S. (1991). The fat tumor suppressor gene in Drosophila encodes a novel member of the cadherin gene superfamily. *Cell* **67**, 853-868.
Maurel-Zaffran, C. and Treisman, J. E. (2000). pannier acts upstream of wingless to direct dorsal eye disc development in Drosophila. *Development* **127**, 1007-1016.
McNeill, H., Yang, C. H., Brodsky, M., Ungos, J. and Simon, M. A. (1997). mirror encodes a novel PBX-class homeoprotein that functions in the definition of the dorsal-ventral border in the Drosophila eye. *Genes Dev.* **11**, 1073-1082.
Morrison, C. M. and Halder, G. (2010). Characterization of a dorsal-eye Gal4 Line in Drosophila. *Genesis* **48**, 3-7.
Murali, D., Yoshikawa, S., Corrigan, R. R., Plas, D. J., Crair, M. C., Oliver, G., Lyons, K. M., Mishina, Y. and Furuta, Y. (2005). Distinct developmental programs require different levels of Bmp signaling during mouse retinal development. *Development* **132**, 913-923.
Oros, S. M., Tare, M., Kango-Singh, M. and Singh, A. (2010). Dorsal eye selector pannier (pnr) suppresses the eye fate to define dorsal margin of the Drosophila eye. *Dev. Biol.* **346**, 258-271.
Panin, V. M., Papayannopoulos, V., Wilson, R. and Irvine, K. D. (1997). Fringe modulates Notch-ligand interactions. *Nature* **387**, 908-912.
Papayannopoulos, V., Tomlinson, A., Panin, V. M., Rauskolb, C. and Irvine, K. D. (1998). Dorsal-ventral signaling in the Drosophila eye. *Science* **281**, 2031-2034.
Pignoni, F., Hu, B., Zavitz, K. H., Xiao, J., Garrity, P. A. and Zipursky, S. L. (1997). The eye-specification proteins So and Eya form a complex and regulate multiple steps in Drosophila eye development. *Cell* **91**, 881-891.
Rawls, A. S., Guinto, J. B. and Wolff, T. (2002). The cadherins Fat and Dachsous regulate dorsal/ventral signaling in the Drosophila eye. *Curr. Biol.* **12**, 1021-1026.
Ready, D. F., Hanson, T. E. and Benzer, S. (1976). Development of the Drosophila retina, a neurocrystalline lattice. *Dev. Biol.* **53**, 217-240.
Reynolds-Kenneally, J. and Mlodzik, M. (2005). Notch signaling controls proliferation through cell-autonomous and non-autonomous mechanisms in the Drosophila eye. *Dev. Biol.* **285**, 38-48.
Riechmann, V., van Crüchten, I. and Sablitzky, F. (1994). The expression pattern of Id4, a novel dominant negative helix-loop-helix protein, is distinct from Id1, Id2 and Id3. *Nucleic Acids Res.* **22**, 749-755.
Sato, A. and Tomlinson, A. (2007). Dorsal-ventral midline signaling in the developing Drosophila eye. *Development* **134**, 659-667.
Sharma, P. and McNeill, H. (2013). Regulation of long-range planar cell polarity by Fat-Dachsous signaling. *Development* **140**, 3869-3881.
Shellenbarger, D. L. and Mohler, J. D. (1975). Temperature-sensitive mutations of the notch locus in Drosophila melanogaster. *Genetics* **81**, 143-162.
Simon, M. A. (2004). Planar cell polarity in the Drosophila eye is directed by graded Four-jointed and Dachsous expression. *Development* **131**, 6175-6184.
Singh, A. and Choi, K. W. (2003). Initial state of the Drosophila eye before dorsoventral specification is equivalent to ventral. *Development* **130**, 6351-6360.
Singh, A., Shi, X. and Choi, K.-W. (2006). Lobe and Serrate are required for cell survival during early eye development in Drosophila. *Development* **133**, 4771-4781.
Spratford, C. M. and Kumar, J. P. (2013). Extramacrochaetae imposes order on the Drosophila eye by refining the activity of the Hedgehog signaling gradient. *Development* **140**, 1994-2004.
Spratford, C. M. and Kumar, J. P. (2014). Dissection of imaginal discs from Drosophila melanogaster. *J. Vis. Exp.* **91**, e51792.
Struhl, G. and Basler, K. (1993). Organizing activity of wingless protein in Drosophila. *Cell* **72**, 527-540.
Strutt, H., Mundy, J., Hofstra, K. and Strutt, D. (2003). Cleavage and secretion is not required for Four-jointed function in Drosophila patterning. *Development* **131**, 881-890.
Sun, X. H., Copeland, N. G., Jenkins, N. A. and Baltimore, D. (1991). Id proteins Id1 and Id2 selectively inhibit DNA binding by one class of helix-loop-helix proteins. *Mol. Cell. Biol.* **11**, 5603-5611.
Tapanes-Castillo, A. and Baylies, M. K. (2004). Notch signaling patterns Drosophila mesodermal segments by regulating the bHLH transcription factor twist. *Development* **131**, 2359-2372.
Thomas, C. and Strutt, D. (2012). The roles of the cadherins Fat and Dachsous in planar polarity specification in Drosophila. *Dev. Dyn.* **241**, 27-39.
Tomlinson, A. and Ready, D. F. (1987). Neuronal differentiation in the Drosophila ommatidium. *Dev. Biol.* **120**, 366-376.
Tomlinson, A. and Struhl, G. (1999). Decoding vectorial information from a gradient: sequential roles of the receptors Frizzled and Notch in establishing planar polarity in the Drosophila eye. *Development* **126**, 5725-5738.
Tsai, Y.-C. and Sun, Y. H. (2004). Long-range effect of upd, a ligand for Jak/STAT pathway, on cell cycle in Drosophila eye development. *Genesis* **39**, 141-153.
Van Doren, M., Ellis, H. M. and Posakony, J. W. (1991). The Drosophila extramacrochaetae protein antagonizes sequence-specific DNA binding by daughterless/achaete-scute protein complexes. *Development* **113**, 245-255.
Van Doren, M., Powell, P. A., Pasternak, D., Singson, A. and Posakony, J. W. (1992). Spatial regulation of proneural gene activity: auto- and cross-activation of achaete is antagonized by extramacrochaetae. *Genes Dev.* **6**, 2592-2605.
Waddington, C. H. and Perry, M. M. (1960). The ultrastructure of the developing eye of Drosophila. *Proc. R. Soc. B Biol. Sci.* **153**, 155-178.
Williams, J. A., Paddock, S. W. and Carroll, S. B. (1993). Pattern formation in a secondary field: a hierarchy of regulatory genes subdivides the developing Drosophila wing disc into discrete subregions. *Development* **117**, 571-584.
Yang, C. H., Simon, M. A. and McNeill, H. (1999). mirror controls planar polarity and equator formation through repression of fringe expression and through control of cell affinities. *Development* **126**, 5857-5866.
Yang, C.-h., Axelrod, J. D. and Simon, M. A. (2002). Regulation of Frizzled by fat-like cadherins during planar polarity signaling in the Drosophila compound eye. *Cell* **108**, 675-688.
Yeung, S. C. and Yip, H. K. (2005). Developmental expression patterns and localization of DNA-binding protein inhibitor (Id3) in the mouse retina. *Neuroreport* **16**, 673-676.
Zeidler, M. P., Perrimon, N. and Strutt, D. I. (1999). The four-jointed gene is required in the Drosophila eye for ommatidial polarity specification. *Curr. Biol.* **9**, 1363-1372.
Zheng, L., Zhang, J. and Carthew, R. W. (1995). frizzled regulates mirror-symmetric pattern formation in the Drosophila eye. *Development* **121**, 3045-3055.
Zhu, W., Dahmen, J., Bulfone, A., Rigolet, M., Hernandez, M.-C., Kuo, W.-L., Puelles, L., Rubenstein, J. L. R. and Israel, M. A. (1995). Id gene expression during development and molecular cloning of the human Id-1 gene. *Brain Res. Mol. Brain Res.* **30**, 312-326.

Supplementary Materials and Methods

PCR Conditions

1.0µl w^{1118} genomic DNA
31.5 µl dH_2O
10.0 µl Phusion Buffer (5X)
3.0 µl Forward primer (0.2 µM final concentration)
3.0 µl Reverse primer (0.2 µM final concentration)
1.0 µl dNTPs (25 mM each)
0.5 µl Phusion DNA Polymerase

Step 1: 98°C 30 seconds
Step 2: 98°C 10 seconds
Step 3: 68°C 30 seconds
Step 4: 72°C 30 seconds/kilobase
Step 5: 72°C 10 minutes
Steps 2 through 4 cycled 35 times

Cloning Strategy

Fragment E1 was amplified from w^{1118} genomic DNA using primers (Listed in Table S1) that added a StuI and XbaI restriction enzyme site to the 5' and 3' end of the fragment sequence, respectively. The amplified PCR product was digested with StuI and XbaI restriction enzymes (NEB Catalog R0187S and R0145S), as was the expression vector placZ-attB. Both the digested fragment region PCR product and the digested placZ-attB vector were purified using the Thermo Scientific GeneJET PCR Purification Kit (Product K0701). The purified, digest placZ-attB vector was phosphatase-treated prior to ligation (NEB Catalog M0289S). The phosphatase enzyme was inactivated by high-temperature incubation but the reaction was not further purified. The digested Fragment E1 PCR product was ligated into the phosphatase-treated placZ-attB plasmid using T4 DNA Ligase (NEB Catalog M0202S). The ligation reaction was used to transform DH5α Subcloning Efficiency Competent Cells (Life Technologies Catalog 18265-017). Cultures were started from the transformation colonies, mini-prepped, and the purified plasmids were sequenced to ensure proper ligation.

Fragments E2 and E3 were both amplified from w^{1118} genomic DNA using primers (Listed in Table S1) that added the Gateway recombination sequences to the 5' and 3' end of the fragment region. The amplified fragment PCR products were cloned into the pDONR201 vector using the Life Technologies Gateway BP Clonase Kit (Product 11789013). The recombined plasmids were used to transform DH5α Subcloning Efficiency Competent Cells (Life Technologies Catalog 18265-017). Cultures were started from the transformation colonies, mini-prepped, and the purified plasmids were sequenced to ensure proper integration of the fragment. The two pDONR201-fragment plasmids were then used to move the enhancer region into the final destination vector pglacZ-attB using the Life Technologies Gateway LR Clonase Kit (Product 11791019). The recombined plasmids were used to transform DH5α Subcloning Efficiency Competent Cells (Life Technologies Catalog 18265-017). Cultures were started from the transformation colonies, mini-prepped, and the purified plasmids were digested to ensure proper integration of the fragment.

Fragment E1 Sequence

CCCATCATGTGTGTGAAATACAATCGTGGATTTCTTGCCCAGAAACCCTGCAACTTCTTCGGTGCAATG
GAGTGGGAGAGAAGTCGAGGCGCCTCGAACTCTTATGTGTGTTCAAGATGTCGTGGACTCAAATTAAG
ATAAGATGCAGATAAGCCGTGCATTTCGATTTAGCCGTTTGAAAACTCGTTAATAAGAATTTGGTCAAT
CCACTGATAACGACTAGTTTTCCATTGAACGGAGGCGCATAACGCTTATCTTTGTTAGGAATAAATATG
ACAAATTGAACGACTACCGTTTAATCGTTTGTCTATATACGAAAACTTAACAGGATTGTTCGAGCTATCA
GTTTATTTGAATAGTTATTGTTAATGAAAACTACTACTAACTAGCCCAATATAATATATTATGAATATTTA
CTCTTCTTATTTTCAAATGATTTAAAATTTTCACCATTCCACAGCGATTAAAATCTAATTTACCCATGCAT
ATATTTAATATTCATTCTGTAATTAATCAAGCCCTTGTTGAACCACTCGCATTGTCTTTTTCGCCTTTTCG
TGTTGATTGTGGAACCTCCTTATCCCACAAAACACTTTTCATTCATTTTCATGCTCATTCACAAAACATG
AGAAAAAAAAAAAGAAAAACAAACATTGCAGTCGTGAGAGGAAAATTATTGAGCGAGAGTTACTGTTCGT
GTTTTCTCATTTTCAGCTGAGAAAAGCAGCCGACCAATCACAAAACCATTTCCCCTTTACAAAAAACCG
ATCATTTTGCATCTCGTGGAGAGTATTCAGATTTGTTTGGAGAGTTTCGGAGAGGAACTCGTTAAGCCG
GGTCTACAAAGGTGAGTATCTGTGGACCGTGGTGGAGTCAGGGGAAATGTTAGTGCTTTAAAAAGTGT
CTACTATGTGTGGAATTTGGATTGTATCTTGTGGATTGGATATTGTGGTAAGGTTGAGTTTCATTTGGTA
TCTCGGGTAGAAGTCAATGAGGTGGATGTTCGGGCACACAGGCTGTAGAACTTGTTGGATATTTTGTC
AAGAACTGAAAGTATCCGAAAGGATTAATTCATAGCATATATACCTCAGTTGTATTTTGAATTATTTTAAA
TTAGTTTTCTCAGAATTCATGGGCTTCACACTACACATCTTCCCCTCTTAAGATCTCAGGCTTAAATTCG
TACTCCATTCTCATTGTGGATTTGAAATGATGACTGTGAAGACCAAACACGAAGGGCTACCCCTTAATT
CCACATTCTTGTCCACCAAAGCAGACCTCTCCGCAACTCACCTCTTAGGAACTCTCCTAAATTCCGGTT
TCAAGTTGTGGTCCAAGTTCCACATGGACACCAATGAGACACATTCCCCAGTCTCCACTCTCCAACCA
AGTACATATCTCTCTCCAGCCGAACGAACCCGAGAGCGAAGACTCCGCCTATCGGATTCGGAAATGCC
CGTTCGGGGGGGTATAAAAGCGGGCGCTCTGAGCGAGCACCACTC

Fragment E2 Sequence

GACTTCTATGTGGCTTCCATCGCAACTATTACTTAGCGCTCCTTTGATGAATATTTTTATGTATATTTTTC
TGCTTCACTAGAATGCTTGACTTATAGTTATTGGTCCCATGATCTGCATACCCCTAACGCAAATCAATC
GGCCCATTGCGAGTCTGAAATCCAGCTGAGCTCGGCAGTTATACCCATGCGTAAACAAAAAAAAAGGC
ATTTCTGTTTCAGTTCCCATTCCCACGCAATTGAGTTTATTGTTTCGCCCGGAGAAAAGGGAAAGGGG
GCGACTGGAGCGAGTAAGTAAACAAAAGCTCAGCGATCATCGACGCCTCAATGGAACTTTTTTTGCTA
CGAAATTAGTATTCAGTTACCATACGGACAACAACAAGTTAAACAAACCTGAAAAAAAAACATGGACACA
GGCCGGATGCGGCTAAAGCAAAAAAAGTCCAAGCCAAGAAGCCTCGACTGCAAGTGGGATCTCTGAT
CTTGGATCACCAATTGCCAATCATCATCGCTGGCCATATGCAAAATATGTTTATAAATAAACGACACTG
AAAGAAGTGGATGTTTACCCAAGTTTCTGCTCAAGATTTAGTTTTAACCGAAATGGTGAAGTGGAGAGC
CTTAAATTTGTGAATGAACTTTATAGTAGTTATAACATTTTGTATTACAGCACTTATCACATGGGCACCA
CAAGATACCATTATATTTCGCAATTGCCACGGGAAGTGTAGAAATTTTTATCGGTGCAGCGAAACGAAA
TCGGTTCCGAATTCCAAGGCGAAGTCATTAATGGGATGTCACTGGAGAGTGACAGGGCAGAGCACCC
CTTTAATGGCAACTAGATGTCCTCAGCCCAGCTGAGATTGGAATGGAATCAGTTCGGCTGGGACTGGG
ATTTCAATGGGGATCGGATCGGATCGGATGGGATCGCATTGGAGATTGGGGCTCGAGGAGCGGGACT
GAGTGACGGGTATTGGATTTCAACATGCAATGCACGCGGCGCGGCATGCGGCTGCATATCTGCAACG
CCATCTCTGGGATACGTCGGGATCCCCTTATCCCCTTATCCCCGATTTCCTATCCCAATATATTATATAT
ATATGAAATACAAAAAAAAAAAAGGCACCGCAAGTGCCCGCCCGCTGATTGACATGTGATCCTCATCTTC
ATCGCATCCTCCACAAGTTTCTATGGCTTGCAAATAGCGGCCCTCTTGCCTTCAGATTTAAATACACTT
TGAATATTAAGTTTATACTTGTGGTATATATTGAATTAAATCGAAGATTCTCAGGAAGTGCATCTTAGAT
ATAGGTAAACCAACTGCAATGCAAACGAACTACAATTTACCATCAGATGTAGGGTATTTAAATTGCGTA
TTTATAGATTTTCTACATTTTTTTCCAGGTTTCTGCTGCTTTTAACCTGTTGTTGGTTCTTCGGCGGCGC
TGCTGATTTGTCATTCAGGCGAAACACTCGCGAGTCGTAAAGTAAGCTCCGTTTCAGTTCCAGTCTCCT
GAAATCTGGCGAAGAAGACGTGAAATCATCTCGAGACGTCGTTGTTGCAGCAGTCATAAAATTATGAT
CGGTATTTTTTAGCCTTCCGTTCCCCTGGGAAATTTGAACTGTGTCGCTGGTTTTTGCCAGCATTTTTTA
GTTATTTCGAGTCTAGTTTTTCGACATGGAACATGGATTTCTGCTGTATTTCATGCAACACCTTGTTCCC
CGATTTCCAGGAACATATGTATGTATGATCTCGGGACATTCCTGAACTGCGTTTCCACGGAAACTTGCA
AATAGACCGTAGTAATTAAAGGCACGAAAGCCGAAGAGCAATAAACACAAGCTTTTCGAGCCCAGTCA
TGTCTCCCATTCAGCCATAGCGAACCAATTCAAAACCATTTCTAACGCAGACGATAACCAGAGAGAGA
CGTGTCGTTTTTCACAAACAACGACGCGCCCGCTCATTTTCAATGAAAATTTCCACAATTTCCTCAATG
GATCGTCGTCGACCCATCATGTGTGTGAAATACAATCGTGGATTTCTTGCCCAGAAACCCTGCAACTTC
TTCGGTGCAATGGAGTGGGAGAGAAGTCGAGGCGCCTCGAACTCTTATGTGTGTTCAAGATGTCGTG
GACTCAAATTAAGATAAGATGCAGATAAGCCGTGCATTTCGATTTAGCCGTTTGAAAACTCGTTAATAA
GAATTTGGTCAATCCACTGATAACGACTAGTTTTCCATTGAACGGAGGCGCATAACGCTTATCTTTGTT
AGGAATAAATATGACAAATTGAACGACTACCGTTTAATCGTTTGTCTATATACGAAAACTTAACAGGATT
GTTCGAGCTATCAGTTTATTTGAATAGTTATTGTTAATGAAAACTACTACTAACTAGCCCAATATAATATA
TTATGAATATTTACTCTTCTTATTTTCAAATGATTTAAAATTTTCACCATTCCACAGCGATTAAAATCTAAT
TTACCCATGCATATATTTAATATTCATTCTGTAATTAATCAAGCCCTTGTTGAACCACTCGCATTGTC

Fragment E3 Sequence

CATTGTTAATCGTATCCTGCGTAATAGCATAATAATCCCTAATCGCATCTGATCAGTTCACCTGGTTGAA
ACACTATCCCTTTCTCTCTCTCGCTCAATTCCCCGTCCCTGTCCCGCACACTATCGAAACGCCGGCTG
CACGATTCCCATTCGCATTACCACTTTGGCTTCCATCGATATGTCCTTTGTGCGCCTTTTGTCGCCGAG
TGTCCTTTTTACCCTAACTACGGGGCTGGGGTTATTTTGACAGCAGTTCATTTGCCTTCTGCCGCCGTT
TTCACTGCTGTTTCACTTTTGGCAAAAACACACAAAAAAAATTTATGAAATTATGCCCAATCCAAATTTA
CAAAATTCAACAAAAATACTTCTATGTGATATAAAAACTTATGAGCTCCATATATATTTCTTTTTGAAACT
GTAAGAATTGCTTCGATATAAATTAGGAATTTATTTCAGTGCAGCTACTCAGCAGTTCGATTGGGGTTTA
AGTTTGGTTTTCCTCTTGAAGCCATGTTTTAGTTTGTTTTATCCTCAATGAGTCGACTTCTATGTGGCTT
CCATCGCAACTATTACTTAGCGCTCCTTTGATGAATATTTTTATGTATATTTTTCTGCTTCACTAGAATGC
TTGACTTATAGTTATTGGTCCCATGATCTGCATACCCCTAACGCAAATCAATCGGCCCATTGCGAGTCT
GAAATCCAGCTGAGCTCGGCAGTTATACCCATGCGTAAACAAAAAAAAAAGGCATTTCTGTTTCAGTTCC
CATTCCCACGCAATTGAGTTTATTGTTTCGCCCGGAGAAAAGGGAAAGGGGGCGACTGGAGCGAGTA
AGTAAACAAAAGCTCAGCGATCATCGACGCCTCAATGGAACTTTTTTTGCTACGAAATTAGTATTCAGT
TACCATACGGACAACAACAAGTTAAACAAACCTGAAAAAAAAACATGGACACAGGCCGGATGCGGCTAA
AGCAAAAAAAAGTCCAAGCCAAGAAGCCTCGACTGCAAGTGGGATCTCTGATCTTGGATCACCAATTGC
CAATCATCATCGCTGGCCATATGCAAAATATGTTTATAAATAAACGACACTGAAAGAAGTGGATGTTTA
CCCAAGTTTCTGCTCAAGATTTAGTTTTAACCGAAATGGTGAAGTGGAGAGCCTTAAATTTGTGAATGA
ACTTTATAGTAGTTATAACATTTTGTATTACAGCACTTATCACATGGGCACCACAAGATACCATTATATTT
CGCAATTGCCACGGGAAGTGTAGAAATTTTTATCGGTGCAGCGAAACGAAATCGGTTCCGAATTCCAA
GGCGAAGTCATTAATGGGATGTCACTGGAGAGTGACAGGGCAGAGCACCCCTTTAATGGCAACTAGA
TGTCCTCAGCCCAGCTGAGATTGGAATGGAATCAGTTCGGCTGGGACTGGGATTTCAATGGGGATCG
GATCGGATCGGATGGGATCGCATTGGAGATTGGGGCTCGAGGAGCGGGACTGAGTGACGGGTATTG
GATTTCAACATGCAATGC

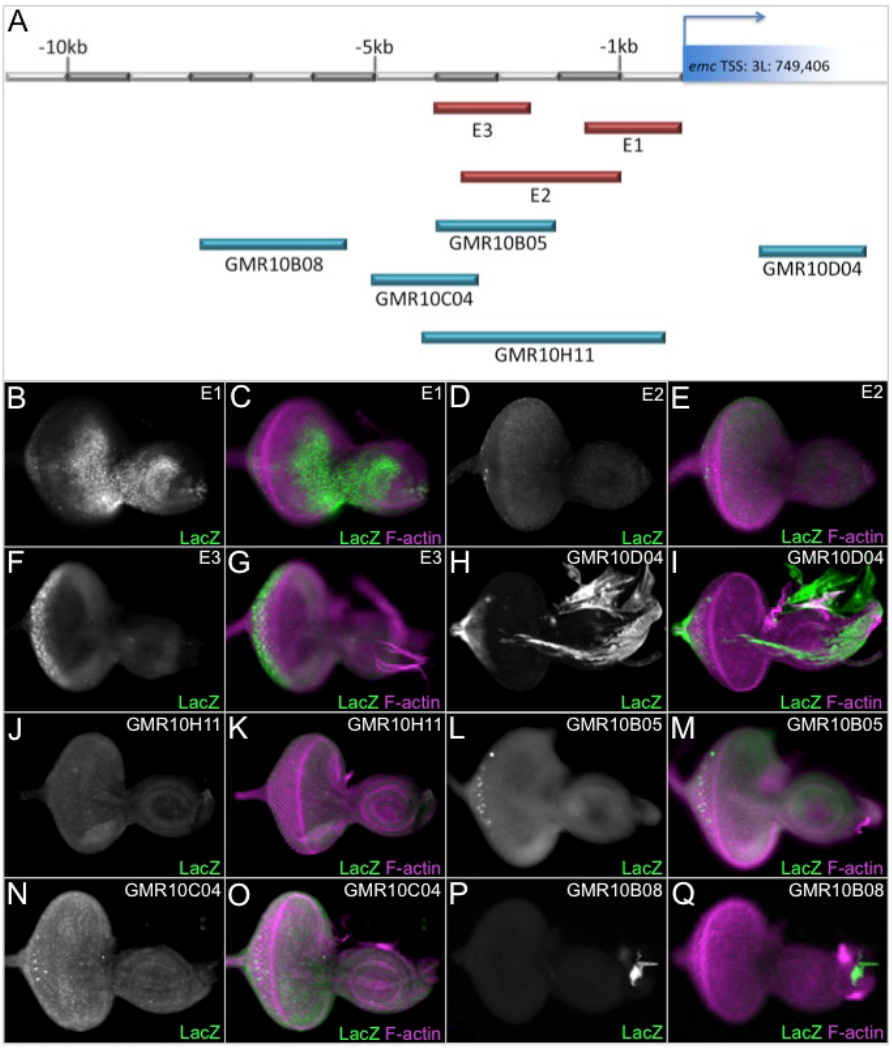

Supplemental Figure 1. Preliminary search for enhancers driving midline expression. (A) Depiction of the genomic region upstream the *emc* transcriptional start site located on 3L and the sub-genomic regions that were tested for the ability to drive expression at the midline. The genomic regions shown in aqua were isolated and fused to GAL4 by Gerald Rubin's laboratory at Janelia Farm. We cloned the regions in red and fused them directly to a lacZ reporter. (B-Q) Expression patterns driven by the eight genomic fragments in early third instar eye discs. None appear to direct reporter expression to the D/V midline. Dorsal side is up and anterior is to the right.

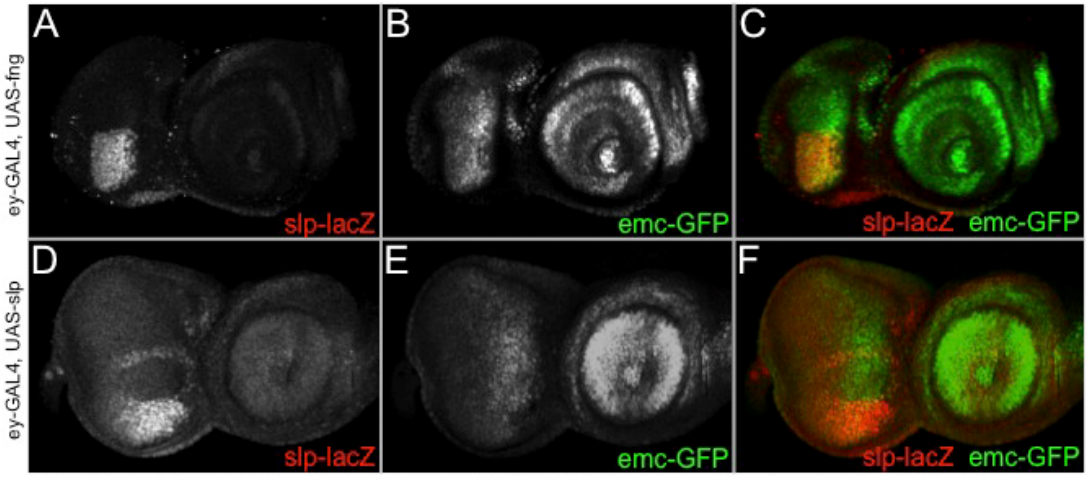

Supplemental Figure 2. Expression of *fng* and *slp* throughout the eye with *ey-GAL4* eliminates enrichment of *emc* expression at the midline. (A-C) Over-expression of *fng* throughout the entire disc using *ey-GAL4*. (D-F) Over-expression of *slp1* throughout the entire eye disc with *ey-GAL4*. In both experiments the enrichment of *emc* expression at the midline is abolished. Dorsal side is up and anterior is to the right.

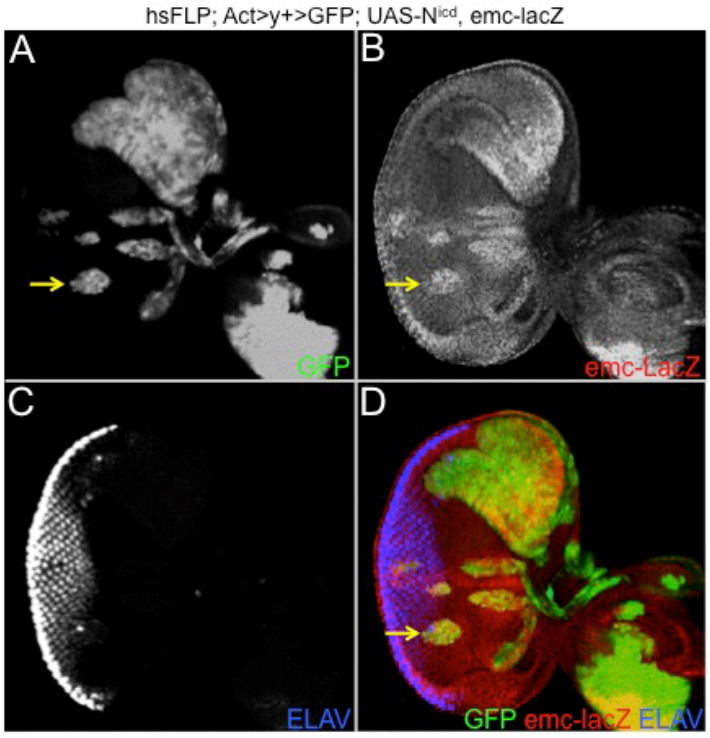

Supplemental Figure 3. Notch signaling can activate *emc* expression. (A-D) Over-expressing the intracellular domain of Notch (*hsFLP/ UAS-N^{icd}; Act>y>GFP/+; emc-lacZ*) in flp-out clones (GFP positive cells in A) show a cell autonomous activation of *emc* expression. Yellow arrow highlights an example of a clone in which *emc-lacZ* is activated in response to higher N signaling. Dorsal side is up and anterior is to the right.

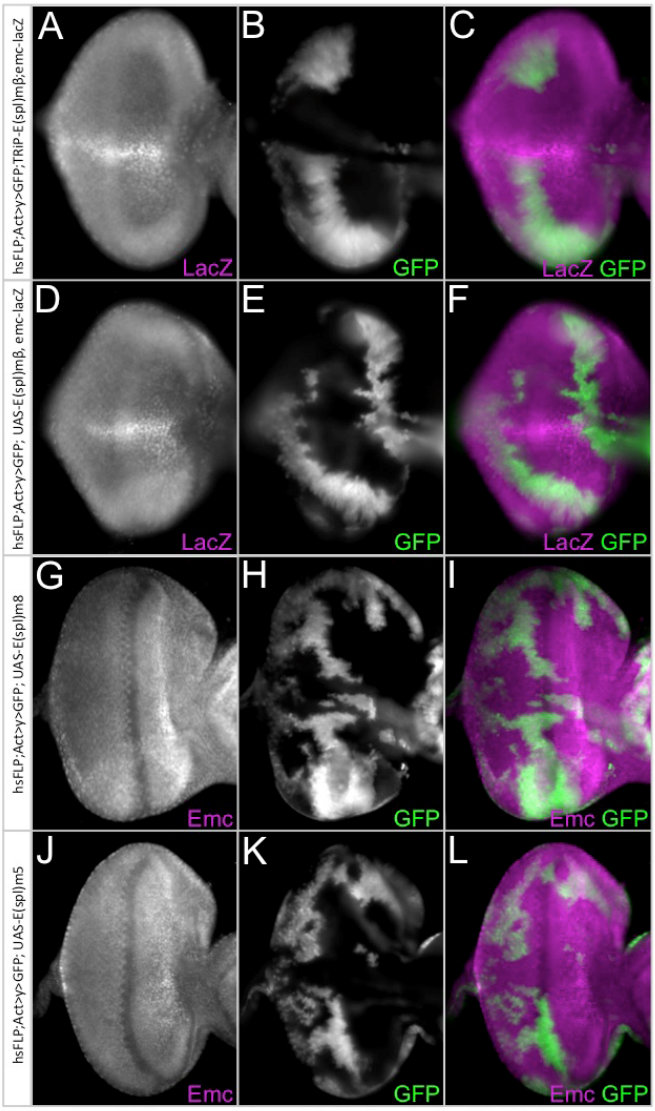

Supplemental Figure 4. *emc* is regulated independently of the E(spl) complex. (A-C) Expression of an RNAi line for *E(spl)mβ* (*hsFLP/+; Act>y>GFP/+; P{TRiP.JF02100}attP2/emc-lacZ*) in flp-out clones (GFP positive cells in B, C) does not alter *emc-lacZ* midline expression. (D-F) Over-expression of *E(spl)mβ* (*hsFLP/+; Act>y>GFP/+; UAS-E(spl)mβ/emc-lacZ*) in flp-out clones (GFP positive cells in E, F) does not alter *emc* levels. (G-I) Flp-out clones of *E(spl)m8* (*hsFLP/+; Act>y>GFP/+; UAS-E(spl)m8/+*: GFP positive cells in H, I) do not affect Emc protein levels in the eye disc. (J-L) Over-expressing *E(spl)m5* (*hsFLP/ UAS-E(spl)m5; Act>y>GFP/+*) in flp-out clones (GFP positive cells in K, L) do not show differences in levels of Emc protein. Dorsal side is up and anterior is to the right.

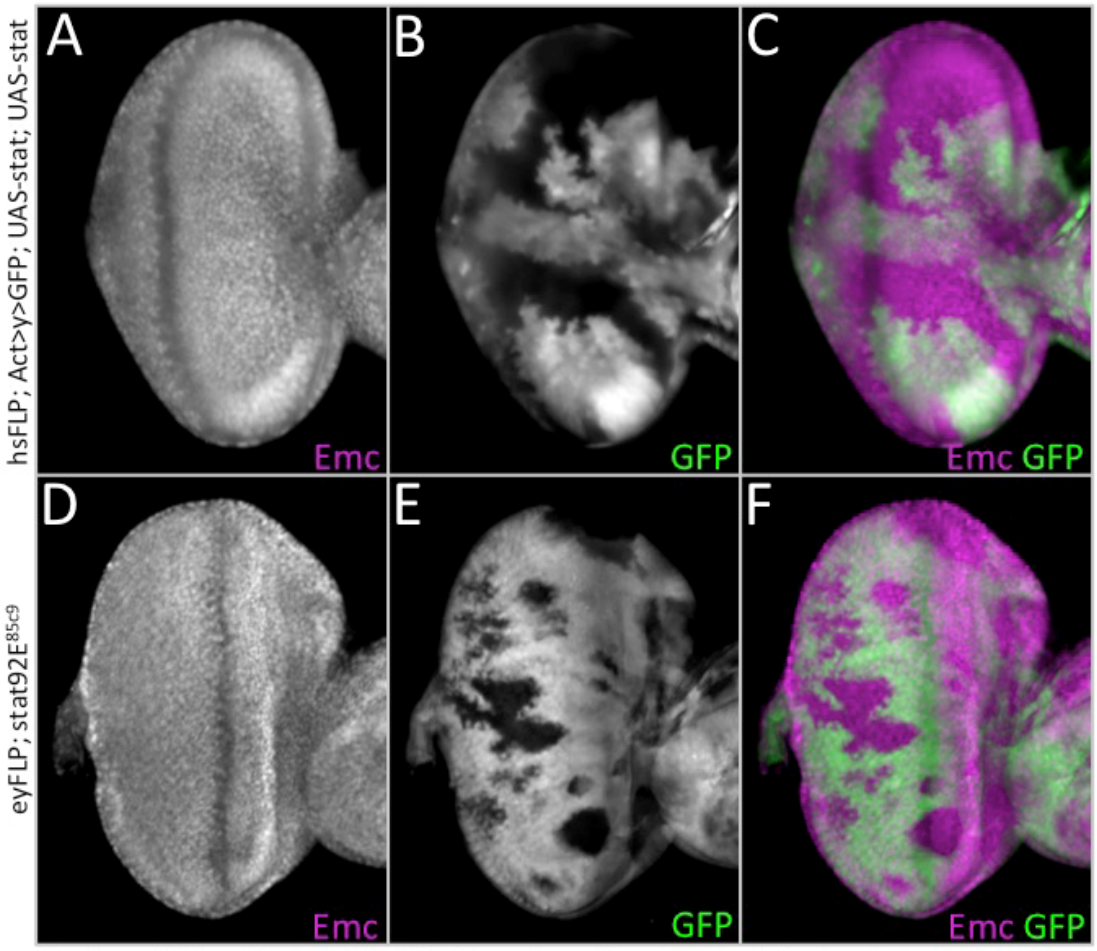

Supplemental Figure 5. The JAK/STAT pathway does not regulate *emc* in the developing eye. (A-C) Over-expression of *stat92E* in flp-out clones throughout the eye field (GFP positive cells in B, C) has no effect on Emc protein levels. (D-F) Mutant clones of *stat92E* (*eyFLP/+; stat92E^{85c9}, FRT82B/Ubi-GFP, FRT82B*) induced throughout the eye (lack of GFP in E) also do not alter normal Emc protein levels. Dorsal side is up and anterior is to the right.

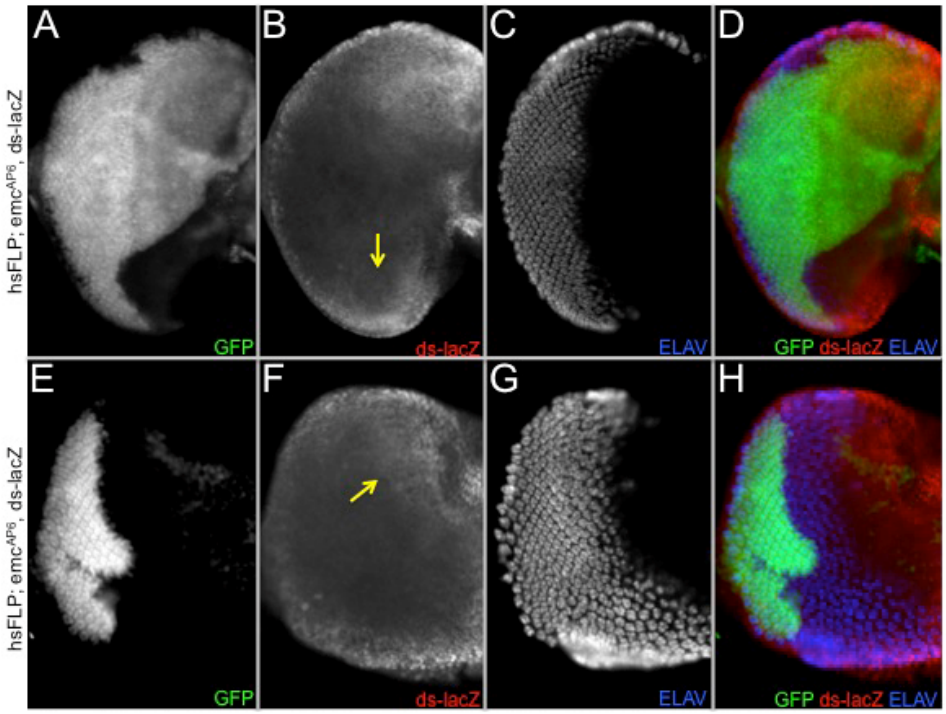

Supplemental Figure 6. Dachsous expression is not regulated by Emc in the developing eye. Two examples in which *ds-lacZ* expression is examined in *emc*^{AP6} loss-of-function clones. (A-D) Ventral *emc*^{AP6} clone, (E-H) Dorsal *emc*^{AP6} clone. At both margins, ds-lacZ expression appears unaffected. Dorsal side up and anterior is to the right.

SUPPLEMENTARY TABLE

Table S1

Click here to Download Table S1